QUANTITATIVE TRACKING OF THE CELLULAR AND SKELETAL RESPONSE OF THE CARIBBEAN CORAL *ORBICELLA ANNULARIS* TO GRADIENTS IN MARINE SEWAGE POLLUTION

BY

ERIN L. MURPHY

THESIS

Submitted in partial fulfillment of the requirements
for the degree of Master of Science in Geology
in the Graduate College of the
University of Illinois at Urbana-Champaign, 2015

Urbana, Illinois

Adviser:

Professor Bruce W. Fouke

Abstract

Orbicella annularis is an abundant framework-building Scleractinian coral that serves as an ecological cornerstone throughout the Caribbean Sea. The *O. annularis* holobiont (all interacting biotic and abiotic components making up the coral) is negatively impacted by increased exposure to anthropogenic pollution, which results in altering coral physiology and increasing the risk of disease infection. Changes in *O. annularis* tissue cellular composition and skeletal structure have been tracked across a 75 km-long gradient from clean to polluted seawater on the fringing reef of the leeward coast of the island nation of Curaçao. A unidirectional ocean current flows to the northwest past the capital city of Willemstad, a large point source of human sewage and ship bilge. Apparently healthy coral colonies were evaluated and sampled by extracting 2.5 cm-diameter biopsies at five sites from Water Plant to Playa Kalki within the back-reef carbonate sedimentary depositional facies. As a result, environmental variables other than pollution, such as water depth, currents, water temperature, oxygenation and other factors remained constant between sites.

Two-photon confocal laser scanning microscopy (TP-LCM) was used for three-dimensional (3D) quantification of the density of zooxanthellae and chromatophore cells within the coral tissues. X-ray computed tomography (BioCT) was used to determine the density of the outermost layer of the coral skeletal being precipitated at the time of sampling in May 2014. Results indicate that zooxanthellae cell tissue densities decreased as pollution concentration increased. Conversely, chromatophore cell tissue densities exhibited no significant covariant changes along the pollution gradient and varied significantly within corals at each site. This implies zooxanthellae cell tissue density is strongly influenced by environmental stress due to pollution,

while changes in chromatophore cell tissue density is controlled by other unknown factors. *O. annulari*s skeletal density showed no significant changes across the geographic pollution gradient, as well as significant within site variations. This suggests skeletal density is not as strongly impacted by pollution as by other unknown biological, physical and chemical factors.

There was a significant positive relationship between chromatophore and zooxanthellae tissue density as well as a negative relationship between chromatophore density and skeletal density. These results have been used to create a new model for healthy coral physiology, integrating the relationship between zooxanthellae, chromatophore and skeletal density of individual *O. annulari*s polyps to better understand their collective role in coral metabolism.

Acknowledgements

This research was funded by the American Association of Petroleum Geologists Grants-in-Aid of Research (AAPG-GIA) program, the Lerner Gray Memorial Fund of the American Museum of Natural History (AMNH), the University of Illinois Urbana-Champaign (UIUC) Graduate College Master's travel award, the Sohl Award for Research Fund and the Evergreen Endowed Fellowship in the UIUC Department of Geology.

I would like to thank the members of the Fouke Lab in the UIUC Carl R. Woese Institute for Genomic Biology (IGB) for their assistance and support with this project. I wish to express a special thank you to Ryanne Ardisana for her guidance, and extensive support at all stages of this project. In addition, I would like to thank Mayandi Sivaguru and Glenn Fried of the UIUC IGB, Lei Lei Yin and Travis Ross of the UIUC Beckman Institute, and Rob Sanford of the UIUC Department of Geology for their invaluable guidance, without which this research would not have been possible. I would like to thank the UIUC Department of Geology for the financial and personal support throughout this research. Finally, I would like to thank my adviser Bruce Fouke for allowing me the opportunity to work on this project, and for supporting me and assisting me throughout this research. His commitment throughout made this possible.

Table of Contents

Chapter One

Introduction

Marine pollution in the form of human sewage, which includes human excrement, wastewater from baths, laundry, sinks and industrial effluent (EPA 2009; Wederfoort 2015), has been shown to have a variety of direct and indirect detrimental impacts on global coral reef health (Knowlton, 2001; Harvell et al. 2004). The organic and inorganic pollutants sourced from sewage, including steroids, metals, pharmaceuticals, inorganic N and P, semi volatile organics and flame retardants (EPA 2009), chemically alter seawater composition. These alterations include increased nutrient and microbial load, and decreased light availability (Lipp et al. 2002; Wederfoort, 2015). Increased nutrient load indirectly impacts coral success by altering planktonic microbial community structure (*bacterioplankton*) and increasing the density of algal competitors (Pandolfi et al. 2005; De'ath and Fabricius, 2010; Vermeij et al. 2010). These components of human sewage pollution have been shown to directly impact the coral animal by decreasing the diversity of microbial communities inhabiting the outermost surface layer of corals (Frias-Lopez et al. 2002; Klaus et al. 2005; Klaus et al. 2007b), decreasing photosynthetic rates of zooxanthellae (Klaus et al. 2007b), increasing susceptibility to bleaching (Goreau and Hayes, 1994) and increasing the prevalence of coral diseases (Buddemeier et al. 2004). These diseases include black band disease (Frias- Lopez et al. 2002; Klaus et al. 2005; Kaczmarsky et al. 2005; Voss and Richardson, 2006; Yang et al. 2014), aspergillosis (Bruno et al. 2003; Baker et al. 2007), yellow band disease (Bruno et al. 2003), and white plague II (Kaczmarsky et al. 2005), among others.

Sewage pollution is just one component of the multifaceted issue of human impacts on coral reef health. Increased sea surface temperature (SST) due to climate change, the most well

studied anthropogenic impact on reef ecosystems, has been linked to both coral bleaching (Berkelmans et al. 2004, McWilliams et al. 2005, Logan et al. 2014), and increasing disease prevalence (Harvell et al. 2002; Buddemeier et al. 2004; Bruno et al. 2007; Miller and Richardson, 2014). The impacts of other anthropogenic stressors such as ocean acidification, nutrient loading, sedimentation, introduction of invasive species, overfishing, and coastal alteration are confounded with sea surface temperature and sewage pollution (Buddemeier et al. 2004; Ban et al. 2014; McClanahan et al. 2014). While coral reefs are impacted by a number of anthropogenic and natural factors, a controlled natural experiment was completed in the field for the present study that allowed for the impacts of one variable to be tested, while all other variables were held constant.

Though human impacts on coral health have been extensively studied over that last few decades, basic questions regarding the effect of sewage impact on healthy coral physiology remain only minimally understood (Klaus et al. 2007; Rosenberg et al. 2007). Coral reefs are complex ecosystems, covering wide swaths of the world's tropical seas from the Tropic of Cancer to the Tropic of Capricorn (Connell, 1978; Spalding et al. 2001). Prior studies quantifying the impacts of sewage pollution on coral physiology have generally focused on a restricted spatial scale without sample sites distributed along a gradient of pollution (Al-Moghrabi et al 2001; Daszak et al. 2001; Kaczmarsky et al. 2005). Utilizing a "Power of Ten" methodical approach, integrating data across large spatial dimensions, to characterize the impacts of sewage pollution on coral health provides a more holistic view of coral response (Fig. 1, Sivaguru et al. 2014). This includes linking ecological impacts on the km-scale of a reef tract, to the μm-scale variation in tissue cell densities.

To have a comprehensive understanding of the impacts of human sewage pollution on *O. annularis*, the coral holobiont must be studied in its entirety. The coral holobiont is defined as all of the living and non-living components comprising the coral colony (Rohwer et al. 2002),

including (1) the coral $CaCO_3$ aragonite skeleton; (2) the cellular components of the coral tissue, including mucocytes, nematocysts, chromatophores (Brown and Bythell, 1995; Houlbrèque and Ferrier-Pagès, 2009); (3) the endosymbiont zooxanthellae (Trench, 1971); (4) the surface microbial layer; and (5) other associated microorganisms, including fungi (Bentis et al. 2000), and nematodes (Raes et al. 2007). Previous studies measuring the impacts of human sewage waste on coral health have primarily focused on surface microbial communities (Rohwer et al. 2001; Lipp et al. 2002; Bourne and Munn, 2005). Coral microbial communities of "apparently healthy" coral, exhibiting no apparent disease, bleaching or physical damage, are distinct from those found within the overlying water column, on the surface of naked skeleton or on the surface of diseased colonies (Frias-Lopez et al. 2002; 2003; 2004). These unique communities play an important role in coral physiology (Rohwer et al. 2002; Klaus et al. 2005) and pathogen defense (Harvell et al. 2007; Shnit-Orland and Kushmaro, 2009). Human sewage pollution has been shown to alter microbial communities, decrease species diversity and increase total microbial density of "apparently healthy" corals (Frias-Lopez et al. 2003; Klaus et al. 2007b). This plays an important role in the risk for many coral diseases, such as Black Band Disease (Frias-Lopez et al. 2002), but it is not the only mechanism by which pollutants alter coral physiology or increase susceptibility to disease and mortality. Klaus et al. (2005; 2007b) provided a more extensive evaluation on the impacts of a gradient of human sewage pollution, along the leeward coast of Curacao, on the *O. annularis* holobiont. Microbial communities exhibited decreased diversity and increased abundance, and zooxanthellae photosynthetic rates decreased with increasing exposure to sewage pollution, while mucus chemical composition and the clade of associated zooxanthellae showed no significant relationship with human sewage. This still provides limited insight into the overall impacts of human sewage on the physiology of *O. annularis* however. More extensive evaluation of the coral

holobiont will provide a better understanding of organism level response to increased sewage pollution.

Recent advancements in instrumentation for optical, biological, mineralogical, and structural analyses have allowed us to image more comprehensively at or below μm-level resolution, with less sample processing necessary than ever before (Helmchen and Denk, 2005; Fouke, 2011; Sivaguru et al. 2012). Previous histological studies have played an important role in our understanding of coral tissue cellular composition, structure, and response to environmental change (Peters, 1984; Peters and Pilson, 1985; Brown et al. 1995; Brown and Bythell, 2005). Recently developed optical microscopy techniques, such as two-photon confocal laser scanning microscopy (TP-LSM), improve histological methods by allowing for optical thin-sectioning to view cellular components, permitting measurements of tissue cell density and three-dimensional distribution of an entire polyp with micron scale resolution (Sivaguru et al. 2014). When excited with a 750 nm laser light source, chromatophores and zooxanthellae emit green and red light respectively, replacing the need for staining, which can further damage these sensitive cells (Sivaguru et al. 2014). Improvements in BioCT scanning allow us to produce 3D skeletal images with μm-level resolution to evaluate density much more efficiently. The combination of these new techniques with more developed methods such as X-raying allow us to more accurately quantify variation within the coral holobiont and study the impacts of environmental stressors on health by providing a more objective control over measurements.

The goal of this study is to quantify the physiological changes occurring in "apparently healthy" colonies of *O. annularis* across a gradient from high to low levels of sewage pollution. This has been accomplished by optically measuring changes in the density and distribution of zooxanthellae and chromatophore cells within the tissues, and the density and width of both high

density bands (HDB) and low density bands (LDB) within the skeletons as indicators. Zooxanthellae were chosen for this study because of their known sensitivity to elevated SST (Hoegh-Guldberg, and Smith. 1989; Davies et al. 1997), and their fundamental importance to coral physiology and metabolism (Trench, 1971; Muscatine 1980; Davies, 1984). Chromatophore density was evaluated because of its assumed role in improving the wavelength of incoming light for zooxanthellae photosynthetically active radiation (PAR) attenuation (Schlichter et al. 1994; Salih et al. 2006). Skeletal density was evaluated because of its sensitivity to changing environmental factors such as SST, and pH (Lough and Barnes, 1997; Hoegh-Guldberg et al. 2007; Holcomb et al. 2014), as well as its importance for structure, strength and carbon dioxide removal within a colony (Chamberlain Jr. 1978; Swart, 1983). Despite our in depth understanding of the coral skeleton, little is known about the direct role tissue physiology plays on skeletal density, and no relationship between skeletal density and human sewage has been previously measured. A baseline for healthy coral tissue and skeletal densities at a pristine site will be used for comparison to assess the response of the coral holobiont to the environmental stresses of raw sewage. The current study provides a baseline for healthy coral tissue and skeletal density at a pristine site with which to evaluate the stress response of *Orbicella annularis* with exposure to varying levels of human sewage pollution. This is quantifiable by changes in density of zooxanthellae and chromatophore cellular tissue and both high and low skeletal density bands, shifting the organism from an autotrophic towards a more heterotrophic lifestyle. Quantifying the direct relationship between human sewage pollution and individual components of the coral holobiont provides a more holistic understanding of the integrative physiological response of an individual colony to sewage pollution.

Chapter Two

Background

O. annularis has been recently reclassified from the genus Montastrea based on evaluation of 11 macro- and 8 micro-morphological, and 11 microstructural characteristics as well as molecular analyses of mitochondrial cox1 (607 bp) and cob (776 bp) DNA sequences (Budd et al. 2012). The oldest relatives of *O. annularis* appeared 5.6 - 3 million years ago in the Seroe Domi formation of Curacao (Knowlton and Budd, 2001), arising prior to the Pliocene-Pleistocene extinction (Budd and Klaus 2001), and are currently abundant, from 1-20 m water depth (Weil and Knowlton, 1994), throughout the Caribbean as far north as Bermuda (Szmant et al. 1997). *O. annularis* precipitates a large aragonite skeleton up to 8 m in diameter and 2 m in height (Szmant et al. 1997), exhibiting columnar morphology with columns widening distally (Knowlton et al. 1992; Knowlton and Budd, 2001). Tissue ranges in color from golden or tan to green (Szmant et al. 1997), with individual polyps, roughly 2 mm in diameter, evenly distributed throughout the coenosarc (tissue interconnecting polyps) (Weil and Knowlton, 1994).

The corallite of *O. annularis* is distinguishable by the small calyx (skeletal cup), with an average width of only 2.34 mm, containing 24 septa (radially arranged plates within calyx) under one mm in length (Fig. 2) (Knowlton et al. 1992). These calices are made up of aragonite needles, ranging from hundreds of nm to a few μm in diameter, produced in acicular bundles, called sclerodermites (Cuif and Dauphin, 1998; Gladfelter, 1983). They are precipitated below the epithelium, growing together in a three-dimensional fan formation around a calcification center rich in sulfated polysaccharides (Cohen and McConnaughey, 2003). A distinguishing characteristic of *O. annularis'* skeletal deposition is the formation of a high and low density band

couplet annually (Knutson et al. 1972; Dodge et al. 1993; Leder et al. 1996; Carricart-Ganivet et al., 2000). Formation of a low density band occurs during low SST (October-June) and the high density band during high SST (July-September) (Barnes and Lough, 1993; Dodge et al. 1993; Carricart-Ganivet and Barnes, 2007). Thickness of these bands is dependent on deposition time causing low-density bands to be wider than high density bands typically (Carricart-Ganivet, 2004; Carricart Ganivet and Barnes, 2007). The formation of density bands is attributed to a response to temperature and carbonate saturation state (Carricart-Ganivet and Barnes, 2007). Both abiotic and biotic processes have been hypothesized to influence band formation. Increased temperature is associated with increased calcification rates, which is hypothesized to be the dominant cause for high density bands in the summer months (Al-Horani 2005; Reynaud et al., 2007). Still it is likely there are large biological controls indicated by the relationship between increased light and increased calcification rates (Kingsley and Watabe, 1985), the 100 fold increase in aragonite saturation state at the site of skeletogenesis compared to surrounding seawater (Tambutté et al., 1996), and enriched skeletal δC^{13} in summer months when respiration rates are high (Swart et al. 2005).

Zooxanthellae are single-celled, dynoflagellate symbionts that inhabit the coral endoderm (Fig. 2), playing an important role in coral physiology (Rowan and Knowlton, 1995; Knowlton, 2001). These cells are able to photosynthesize using CO_2 derived from coral respiration, providing the coral animal with orders of magnitude more energy, via glucose production, than heterotrophy alone allows (Trench 1971; Muscatine et al. 1981; Hallock 2001; Swart et al. 2005). In return, the coral provides inorganic nutrients, a consistent source of carbon and a controlled environment for the zooxanthellae, with protection from predators and UV radiation (Shashar et al. 1997). This relationship has played an important role in Scleractinian coral evolution, providing them the

ability to hypercalcify, excrete a rigid skeleton from $CaCO_3$ extracted from sea water (Constantz 1986; Stanley, 2003), and restricting them to shallow, nutrient depleted tropical ecosystems (Budd et al. 1996; Cohen and McConnaughey, 2003; Stanley Jr, 2006).

Chromatophores are a light manipulating cell found within the tissue of many marine invertebrates with varying roles depending on host species (Schlichter et al. 1985; Messenger 2001; Nowack et al. 2008). The exact role of chromatophores within Scleractinian coral tissues is uncertain, and two hypotheses have been proposed (Schlichter et al. 1994; Salih et al. 2000). One hypothesis suggests the primary role of chromatophore cells is to lengthen the wavelength of high-frequency incident light to that which can be better utilized by zooxanthellae for photosynthesis (Schlichter et al. 1986; 1994). By improving efficiency of light attenuation, this would increase inhabitable depth range, and lengthen the period during which zooxanthellae can photosynthesize daily (Schlichter et al. 1994). The second hypothesis suggests that chromatophores function to protect corals from light damage by reflecting harmful, unusable radiation (Salih et al. 2000). This would protect zooxanthellae and photosynthetic machinery from UV damage, allowing them to inhabit shallow marine waters to depths of less than a meter (Weil and Knowlton, 1994). It has more recently been suggested that chromatophores are able to take on both physiological functions, acting as photo-protectors in high light intensity and photo-enhancers in low light (Dove et al. 2001; Salih et al. 2006). Likely, there is variation between both species and environment. More controlled, laboratory and field experimentation is required to understand the role of chromatophores in *O. annularis.*

Chapter Three

Materials and Methods

Geobiological Setting and Characterization of Study Sites

The Caribbean island of Curacao is the ideal location for *in situ* experimentation on the impacts of a gradient in marine sewage pollution on a coral reef tract (Fig. 3). The capital city of Willemstad is home to approximately 80% of the nation's population and is a focused point source of human sewage pollution (Gast 1998a; Klaus et al. 2007). The primary effluent sewage pipeline transports untreated sewage from the municipal sewage plant at 12.106342, -68.941677 to the ocean at Boca Simon where it mixes with coastal waters (Sulvuran, 2014). Approximately 10,000 m^3 of sludge, containing nutrients, metals, hydrocarbons, and industrial chemicals, are released daily (Gast 1998a, b).

The unidirectional oceanographic current flowing to the northwest along the southern margin of Curacao passes Willemstad, creating a gradient of human sewage pollution as the sewage is mixed and diluted with fresh seawater (Gast 1998a; Klaus et al. 2007). Quantifying this relationship can prove challenging, however seawater $\delta^{15}N$ content has been shown to adequately reflect the concentration of a sewage pollution (Heikoop et al. 1998; 2000a, b). Human sewage is generally enriched in $\delta^{15}N$, due to bacterial transformation of dissolved inorganic nitrogen from human sewage through denitrification (reduction of NO_3^-, NO_2^-, NO or N_2O to N_2), nitrification (oxidation of ammonia to nitrite), and nitrogen fixation (N_2 conversion to ammonium) (Swart et al. 2005; Klaus et al. 2005). Coral integrates $\delta^{15}N$ into its tissue at rate proportional to seawater concentration. With regular sea water mixing, an increased distance from the point source of sewage pollution is characterized by a decrease in $\delta^{15}N$ of coral tissue (Fischer et al. 2013). Coral

tissue $\delta^{15}N$ of "apparently healthy" *O. annularis* was measured at five sites along Curacao's southern coast, Boca Simon, Water Plant, Snake Bay, Playa Hundu, and Jan Thiel (Fig. 3). The $\delta^{15}N$ tissue concentration was highest at Boca Simon and decreased with distance from the point source of human sewage (Fig. 4). Low $\delta^{15}N$ values measured at Jan Thiel suggest seawater southeast of the Boca Simon sewage effluent is relatively pristine (Klaus et al. 2005).

To assess the impacts of human sewage pollution on the coral holobiont, three "apparently healthy" *O. annularis* colonies at least 1 meter in diameter, were sampled from five sites along a gradient of impact, Jan Thiel (12.073774, -68.878463), Playa Kalki (12.375333, -69.158882), Reef Marie (12.218514, -69.085878), Snake Bay (12.139423, -68.997379), and Water Plant (12.109514, -68.954179). Jan Thiel, Snake Bay and Water Plant were chosen because of known $\delta^{15}N$ values. Reef Marie is located roughly two miles SE of Playa Hundu and was sampled instead for ease of access. Playa Kalki, the furthest downstream locale, was sampled to represent a return to pristine conditions. All colonies were sampled at approximately 5 meter water depth from within the back reef depositional facies (Fig. 5). A depositional facies represents a sedimentary rock formation characterized by the physical, chemical and biological environmental processes occurring during the time of deposition (Reading, 1996; Fouke et al. 2001; Fouke et al. 2011). The sampling of coral colonies within a facies context, ensures a controlled, comparative baseline for evaluating the impacts of human sewage pollution without variation in other influential environmental factors (Fouke et al. 2011).

Seawater temperature and water depth were measured adjacent to each coral colony using an Oceanic Veo100 dive computer. Ten ml falcon tubes were flooded with seawater directly above each colony and pH was measured upon return to the beach using Hydrion pH 6-8 strips. Photosynthetic active radiation (PAR) was measured using a Li-Cor PAR unit with a Li-192

Underwater Quantum Sensor. Three measurements were taken at the water's surface, immediately before descending for the sampling dive. Three measurements were taken laterally adjacent to each coral colony prior to sampling, with the sensor pointing directly towards the water's surface. Measurements were normalized by calculating PAR near each colony as a percentage of PAR at the water's surface.

Coral Tissue-Skeleton Biopsy Collection

Standard compressed air SCUBA diving techniques were used to collect two biopsies from each colony using a McMaster-Carr steel core punch, 2.5 cm in diameter, which was thoroughly rinsed in seawater between each use (Fig. 6). The core punch was driven through the tissue approximately 4 cm into the skeleton using a rock hammer, and removed slowly from the colony with the biopsy. The biopsy was then gently removed from the core punch and placed in a sterile 50 ml Falcon centrifuge tubes tube flooded with seawater. Upon return to the beach, seawater was decanted and biopsies were immediately transferred to appropriate fixatives. Skeletal biopsies were stored in 70% EtOH at room temperature. Tissue samples were stored in Formalin (9:1 diH_2O: Formaldehyde) at 4^oC in dark, insulated Igloo cooler. All samples were placed in a Styrofoam test tube holder wrapped tightly with Saran wrap and stored on icepacks within the cooler for transport to the University of Illinois, where further processing and analysis took place.

Three-Dimensional (3D) Analysis of Coral Tissue Cellular Composition and Structure

Tissue samples were imaged using two-photon confocal laser scanning microscopy (Zeiss TP-LSM710) housed at the Institute for Genomic Biology, University of Illinois at Urbana-Champaign (Sivaguru et al. 2014). Both chromatophores and zooxanthellae exhibit auto-

fluorescence under 780 nm wavelength UV excitation, emitting green light at 500 nm and red light at 675 nm respectively. This method requires no further tissue fixation or alteration which may impact measured cell densities. Intact coral biopsies were imaged at 20x zoom. The tile scan mode was used to image half of a polyp collecting 24 tiles (4x6) per plane. Samples were optically thin-sectioned, with images taken every 10 μm moving through the z-plane to ensure no cells were missed or double counted when the 3D tissue samples were reconstructed (Sivaguru et al. 2014).

IMARIS, produced by Bitplane, was used to recreate the 3D image of the coral polyp (Fig. 7). The chromatophore and zooxanthellae cell densities of five secondary septa, chosen from three polyps per colony were measured to represent average tissue cell density for each colony (Fig. 8). Secondary septa were used, because they had the same densities as adjacent primary septa but exhibited less damage associated with sample collection. To measure cell density in each septa, the 3D volume of the entire polyp was recreated by compiling the z-stack of all the images. The reconstruction was cropped to isolate an individual secondary septa. The chromatophore and zooxanthellae tissue volume were then reconstructed using optimal thresholding selecting for pixels of the appropriate color. Cell density was parameterized as the volume of each cell over the total volume of the secondary septa analyzed. Tissue cell density provided for each colony is an average of all analyzed secondary septa tissue density. The tissue cell density for each locale is calculated as an average of all 15 secondary septa analyzed from that site.

Three-Dimensional (3D) Analysis of Skeletal Structure and Density

Tissue was gently washed off skeletal samples using a lab sink on high pressure to avoid any damage to the skeleton. A 5 mm-thick section was cut from the middle of each skeletal biopsy using an Edco Tile Saw at the Natural Resource Studies Annex, University of Illinois at Urbana-

Champaign. Thick sections were dried in a Fisher Scientific laboratory oven at 60 ^{o}C for 24 hours. Skeletal samples were imaged on a GE Proteus System Console X-ray machine (2D spatial resolution of 160 um) housed at the School of Veterinary Medicine, University of Illinois at Urbana-Champaign. These images were used for locating skeletal density bands when analyzing 3D reconstructions.

Three-dimensional (3D) images of skeletal samples were taken using an Xradia BioCT scanner housed at the Beckman Institute, University of Illinois at Urbana-Champaign. Samples were imaged using a 1x zoom yielding a 3D spatial resolution of 16 µm. The sample was rotated 360^{o} and a total of 901 images were taken. The program XMController was used to control imaging settings. The 2D images were compiled into a 3D reconstruction and shift and hardness were altered manually using XMReconstructor.

Amira, produced by Field Emission Inc., was used for image analysis (Fig. 9). The optimal threshold was manually selected in the xy, yz, and xz planes (z being distance from the growing surface) for 3D skeletal reconstruction. Each reconstruction was cropped so only intact, undamaged skeleton was included in density analysis. Total skeletal volume per slice and total slice volume were measured for each 2D slice in the z plane. This allowed us to distinguish between the total densities of each growing layer. The high density bands (HDBs) and low density bands (LDBs) were located using 2D X-rays taken as a guideline. Density bands from the same growth year were analyzed for each sample. The density for 20 consecutive slices (0.2 mm), from the most recently deposited HDB (closest to growing surface), were averaged to estimate total density for the HDB. The same was done to calculate average density for the most recently deposited LDB, and the density of the growing surface was average for the top 0.5 mm (50 consecutive slices).

Two-Dimensional (2D) Analysis of Skeletal Structure and Density

The Xradia BioCT scanner at the Beckman Institute, University of Illinois was used for high resolution two-dimensional (2D) skeletal imaging. One image for each skeletal thick section was taken at 0.5x zoom, yielding a spatial resolution of 14 μm per pixel. XMController and XMReconstructor were used to control imaging settings and reconstruction respectively.

Fiji, an image J product, was used for 2D skeletal analysis. Each image was cropped around the skeleton to increase internal contrast. Next, a fast-fourier transformation (FFT) plot of the image was created and the noise in images due to vertical bands was manually removed. The inverse FFT produced showed only the horizontal, seasonal density bands of interest. Image properties were converted from pixels to microns. Two 200 μm transects were analyzed for gray-scale values from each sample. Gray scale values of less than one were associated with LDBs and greater than or equal to one with HDBs. The width of the high density bands closest to the growing surface and the distance to the first HDB were calculated for each transect using gray-scale graph and table values (Fig. 10). Calculated widths for each transect were averaged to estimate the HDB width and distance from the growing surface to the first HDB within each sample.

Chapter Four

Results

Sampling Site Environmental Conditions

The fringing coral reef ecosystems at Jan Thiel, Water Plant, Snake Bay, Reef Marie and Playa Kalki (Fig. 11) appeared healthy and productive, exhibiting high extents of seafloor coral coverage that were consistent with previous detailed ecological surveys conducted for each site several decades ago (Bak et al. 1977; Bak and Luckhurst, 1980; Van Duyl 1985). The exception being the underrepresentation of *Acropora palmata* and *A. cervicornis* due to population declines associated with white band disease (Aronson and Precht, 2001). Sites were grouped into three distinct types, (1) upstream low-impact normal marine at Jan Thiel; (2) high impact non-normal marine at Boca Simon and Water Plant; and (3) a gradient from impacted to normal marine from Snake Bay to Playa Kalki. Seawater temperature (26^{o}C) and pH (7) were constant at all sites (Table 1), while the water depth at which sampled *O. annularis* colonies were growing was as constant as possible at 5.9 to 8.3 m. The reefs at Jan Thiel, Snake Bay, Reef Marie and Playa Kalki exhibited a high diversity of coral species, dominated by *Orbicella, Diploria, Millepora and Porites spp*, which is expected under normal marine conditions (Van Duyl, 1985; Bak and Nieuwland 1995; Bruckner and Bruckner, 2006; Edmunds and Elahi, 2007). Conversely, the reef at Water Plant exhibited relatively low species diversity dominated by *Diploria strigosa*, similar to that of Boca Simon described by Van Duyl (1985). Furthermore, the reefs at Playa Kalki and Reef Marie were directly offshore from resorts that had constructed artificial beaches, with ensuing offshore sand transport impacting the reef health in both areas, exhibited by decreased colony abundance (Reef

Marie: 50%, Playa Kalki: 80% when compared with Jan Thiel) and size (predominately <1 meter) with increased algae cover (Fig. 11).

Zooxanthellae Tissue Cell Density

Zooxanthellae tissue cell density did not vary significantly between colonies found at the same locale (Table 2). Zooxanthellae tissue cell density was negatively correlated with human sewage pollution (Fig. 12). Jan Thiel, the upstream low-impact normal marine environment, had a significantly higher zooxanthellae tissue cell density (22.7 ± 1.67) than all other locales (Table 3). Zooxanthellae tissue cell density was lowest at Water Plant (14.5 ± 1.23), the high impact non-normal marine environment. Zooxanthellae cell densities at Snake Bay, Reef Marie and Playa Kalki, a gradient from impacted to normal marine, were all significantly lower than Jan Thiel and greater than Water Plant (Table 4). Zooxanthellae cellular density at Snake Bay (16.6 ± 1.69) was less than at Reef Marie (16.7 ± 1.05), but greater than at Playa Kalki (15.2 +/- 1.04) (Fig. 12).

Chromatophore Tissue Cell Density

There was no evident relationship between concentration of human sewage pollution and chromatophore tissue cell density (Fig. 12). Chromatophore tissue cell density at Jan Thiel (5.11 ± 0.736), the upstream low-impact normal marine, and Water Plant (6.17 ± 0.781), the high impact non-normal marine environment showed no significant variation (Table 3). Chromatophore tissue cell density only varied significantly at one site along a gradient from impacted to normal marine, at Snake Bay (11.3 ± 1.25). Both Playa Kalki (4.47 ± 0.525) and Reef Marie (4.68 ± 0.941) showed no significant variation from other locales. There were significant differences in chromatophore

density of different colonies (Table 2) from the same locale at Jan Thiel, Water Plant, Snake Bay, and Reef Marie (Table 5).

Density of High and Low Skeletal Density Bands

There were no significant differences in HDB or LDB skeletal density between any of the sampled sites (Fig. 13), however large variations existed in both HDB and LDB density of different colonies from the same locale, experiencing the same abiotic conditions. Average HDB skeletal density (Table 6) at the low impact, normal marine environment, Jan Thiel, was 67.18% with a range of 10.31%, while average LDB skeletal density (Table 7) was 54.74% with a range of 10.14%. Average HDB skeletal density in a high impact non-normal marine environmental, Water Plant, was 68.15% (range: 17.42), and average LDB skeletal density was 57.72% (range: 9.05). Average HDB skeletal density of three colonies could only be calculated at one site along a gradient from impacted to normal marine, Reef Marie (74.64%, range: 5.99). There was no significant variation in LDB skeletal density along a gradient from impacted to normal marine. Average LDB skeletal density for Reef Marie was 63.45 (range: 3.85), Snake Bay was 56.3 (range: 1.85), and Playa Kalki was 55.34 (range: 11.18).

Comparative Chromatophore and Surface Skeletal Density

The linear correlation between average chromatophore cell density and skeletal density at the growing surface (top 0.5 mm) for all 15 colonies sampled (Table 9) has an associated R-value of -0.478, indicating a negative correlation between the two variables, with a significant one-tailed p-value of 0.036 (Fig. 14).

Skeletal Density Band Width

There was no significant relationship between HDB width and concentration of human sewage pollution, however large variations existed in HDB width of different colonies from the same locale (Fig. 15). Average HDB width (Table 8) at the low impact normal marine environment, Jan Thiel (1152 μm), and the high impact non-normal marine environment, Water Plant (1173.33 μm), showed no significant difference. Average HDB width along a gradient from impacted to normal marine environments, Snake Bay (1117.33 μm), Reef Marie (884 μm), and Playa Kalki (860 μm), showed no significant variation. Intra-site HDB width varied dramatically at all five locales, with the greatest range in HDB width of 1008 μm measured at Jan Thiel (Water Plant: 608 μm, Snake Bay: 752 μm, Reef Marie: 528 μm, Play Klaki: 984 μm).

Chapter Five

Discussion

The systematic changes in coral tissue $\delta^{15}N$ documented by Klaus et al. (2005) provides an environmental baseline against which changes in coral physiology and cellular structure can be quantitatively gauged. Human sewage is generally enriched in $\delta^{15}N$, due to bacterial transformation of dissolved inorganic nitrogen from human sewage through denitrification (reduction of NO_3^-, NO_2^-, NO or N_2O to N_2), nitrification (oxidation of ammonia to nitrite), and nitrogen fixation (N_2 conversion to ammonium; Swart et al. 2005; Klaus et al. 2005). With regular sea water mixing an increased distance from the point source of sewage pollution is characterized by a decrease in $\delta^{15}N$ of coral tissue. The increase in the δ15N of *O. annularis* tissue with increased proximity to Boca Simon indicates apparently healthy *O. annularis* colonies are consuming and assimilating human sewage pollutants into their tissue (Klaus et al 2005). Jan Thiel, the low-impact, normal marine environment, had the most apparently healthy reef tract, exhibited by the greatest species diversity and large colony size. Reefs along a gradient from impacted to normal marine exhibited intermediate reef health. Snake Bay exhibited large colony size and intermediate species diversity, dominated by *Orbicella* species and *D. strigosa.* Both Reef Marie and Playa Kalki were characterized by intermediate species diversity, with *Orbicella* species and *D. strigosa* dominating. The presence of artificial sand beaches along the back reef seemed to increase algal cover and decrease colony size within the back reef facies. Apparent health was lowest at the impacted non-normal marine reef, Water Plant, characterized by lower species diversity, and a community dominated by *D. strigosa.* The reef community of Boca Simon, characterized by Van

Duyl (1985), showed low species diversity, and reefs dominated by *Diploria* and *Orbicella* species very similar to that of Water Plant both then and today.

Apparently healthy *O. annularis* colonies were present at all sites, but physiological variation exists between colonies exposed to different concentrations of human sewage pollution. Human sewage pollution has previously been shown to cause an increase in coral disease and mortality (Bruno et al. 2003; Buddemeier et al 2004; Yang et al. 2014). The impacts of human sewage pollution on surficial microbial communities has been extensively studied (Lipp et al. 2002; Frias-Lopez 2003; Klaus et al. 2005; Kline et al. 2006). The sewage effluent being released at Boca Simon has been shown to alter the microbes inhabiting the surface of corals by decreasing diversity of microbial communities, and increasing abundance (Klaus et al. 2005). This shift in the microbial communities of apparently healthy corals with pollution exposure is also evident in the transition between healthy and diseased colonies (Fig. 16) suggesting changing communities may be associated with increased infection rates (Frias-Lopez et al. 2002; Klaus et al. 2005). Furthermore, exposure to human sewage pollution along the Curaçao reef tract has resulted in a decrease in the zooxanthellae photosynthetic activity in *O. annularis* (Klaus et al. 2007). The present study builds directly upon these findings, adding quantitative analyses of changes in the cellular and skeletal composition of *O. annularis* across the Curaçao reef tract pollution gradient.

Impacts of Sewage Pollution on O. annularis Zooxanthellae Tissue Cell Density

Zooxanthellae tissue cell density was significantly greater at the low-impact normal marine site, Jan Thiel, than all sites located downstream of Boca Simon, impacted by human sewage pollution (Fig. 12). The lowest zooxanthellae tissue cell density was found at the high-impact, non-normal marine environment, Water Plant. This indicates an increase in human sewage pollutant

concentration decreases the success of zooxanthellae within the coral tissue. Zooxanthellae tissue cell density at all sites along a gradient from impacted to normal marine, Snake Bay, Reef Marie and Playa Kalki, were greater than at the high, non-normal marine environment but lower than at the low-impact normal marine site. A similar response was exhibited with exposure to other pollutants including, cyanide (Cervino et al. 2003), and heavy metals (Goh and Chou, 1997), while other studies suggest some pollutants, such as nitrate, increase zooxanthellae density (Marubini and Davies, 1996). This implies zooxanthellae tissue density decreases as the tissue environment becomes less suitable for their success. The same relationship is seen with increased sea surface temperature (Goreau and Hayes, 1994; Brown 1997; Loya et al. 2001; Hoegh-Guldberg 1999). In situations of extreme thermal stress, this is visible as coral bleaching (Glynn 1996; Downs et al. 2002; Berkelmans et al. 2004). Our results suggest that zooxanthellae density can be significantly lower without visible bleaching however.

The evolutionary success of frame-work building corals, such as *O. annularis*, has been driven by their coevolution with zooxanthellae (Stanley and Swart, 1995). Many studies have shown loss of zooxanthellae due to thermal bleaching has been associated with increased risk of disease and increased mortality rate (Kuta and Richardson, 2002; Miller et al. 2006; Muller et al. 2008; Thornhill et al. 2011). The longer coral suffers from bleaching the greater their vulnerability to disease becomes (Toller et al. 2001; Brandt and McManus, 2009). Input of pollution on the southern coast of Curacao is consistent, suggesting lower zooxanthellae density is maintained throughout the year. It is possible maintaining low zooxanthellae density consistently would increase risk of disease without evident bleaching, but further controlled studies would be needed support this.

Impacts of Sewage Pollution on O. annularis Chromatophore Tissue Cell Density

Our results suggested there was no significant relationship between pollution and chromatophore density (Fig. 12). We expected chromatophore density to decrease with increased exposure to human sewage. This is because loss of zooxanthellae would encourage a shift to a more heterotrophic lifestyle. If the dominant role of chromatophores is in improvement of zooxanthellae light attenuation (Schlichter et al. 1994), then we would expect coral to allocate less energy to chromatophore production and allocate more energy to heterotrophy.

Though there were was no clear relationship between pollution level and chromatophore density, significantly higher chromatophore tissue density was measured at Snake Bay. It is possible this is related to unique environmental conditions. Variation in chromatophore density has been shown to vary with water depth (Schilchter et al. 1994; Salih et al. 2000). However, temperature, pH, PAR and sampling depth were consistent across all five sites and Snake Bay has an intermediate level of human sewage pollution. Intra-site variation in chromatophore tissue cell density was significant at Water Plant, Jan Thiel, Snake Bay and Reef Marie. Abiotic conditions at each site are assumed to be consistent, with some colonies sampled only a few meters apart. This suggests phenotypic variation may play a more important role in chromatophore density than environment. These variations could be genetic, epigenetic, or related to a colony's life stage.

Previous studies evaluating the role of chromatophores have focused on variation in chromatophore tissue cell density between colonies across changing environmental conditions (Schlichter et al. 1994; Salih et al. 2000). If variation in chromatophore tissue cell density is primarily dependent on biological differences between the colonies rather than environment, studies comparing chromatophore density across environmental gradients may not be effective for evaluating their physiological role (Schlichter et al. 1985; Schlichter et al. 1994; Salih et al. 2000).

To understand the role of chromatophores in coral physiology, future research should focus on long-term field studies of the same colonies, and controlled experimentation on fragments from the same colony. Additionally, more extensive proteomic analyses could help quantify chromatophore activity.

Impacts of Sewage Pollution on O. annularis Skeletal Growth

There was no significant difference in HDB or LDB skeletal density, or HDB width at any of the sites evaluated, and therefore no clear relationship with human sewage pollution (Fig. 13, Fig. 15). Decreased skeletal density due to increased water acidity has been associated with weakening of the coral holobiont (Hoegh-Guldberg et al. 2007; Cao et al. 2007). This suggests that though increased acidity can alter skeletal density, human sewage pollution of neutral pH does not likely have direct impacts on coral skeletal density. Many aspects of skeletal growth were not measured in this study however, including growth rate. Relationships between zooxanthellae density and growth rate have been identified (Goreau and MacFarlane, 1990). Because zooxanthellae density decreases with increased exposure to human sewage pollution, it is possible that growth rate varies while density is maintained. Long-term growth studies and skeletal imaging would be necessary to evaluate this.

It is possible a relationship between skeletal growth and human sewage exists, but was not evident due to the small sample size of three colonies per site. Historically, variation in skeletal density band growth has been attributed primarily to changes in temperature, carbon saturation state, and pH (Marshall and Clode, 2004; Cooper et al. 2008), however none of these seemed to vary significantly between sites. Interestingly, the intra-site variation in colony skeletal density, both of HDBs and LDBs, at the same locale was large. Previous studies have suggested variation

in skeletal density is driven primarily by abiotic conditions (Highsmith, 1979; Barnes and Lough, 1993), however we measured variations of greater than 15% between density bands from the same depositional period of different colonies exposed to the same abiotic conditions. This suggests there is a biotic control impacting skeletal density as well. It has been previously suggested that skeletal density is influenced by coral metabolism with higher density bands produced when colonies are more heterotrophic and need to remove excess metabolic CO_2, and lower density bands produced when zooxanthellae are consuming excess CO_2 for photosynthesis (Marubini and Davies, 1996; Gattuso et al. 1999; Swart et al. 2005). We suggest the formation of density bands are primarily driven by abiotic conditions, however variation seen between skeletal band densities of different colonies within the same deposition period are controlled by metabolic CO_2 availability. Future studies should use fragments from the same colony in controlled environmental conditions to better understand the role of environmental impacts on skeletal growth.

Integrating chromatophore and skeletal density

The correlation between chromatophore tissue cell density and skeletal density at the growing surface (top 0.5 mm) suggests 22.8% of variance in skeletal density can be associated with the chromatophore tissue cell density of the colony. This significant negative correlation indicates that as chromatophore density increases, skeletal density decreases. This supports the hypothesis of Schlichter et al. (1994) suggesting chromatophores of *O. annularis* play a role in improving zooxanthellae light attenuation. When colonies experience the same amount of available light, those with greater chromatophore density would be more photosynthetically efficient. As previously stated, it has been hypothesized that increased rates of photosynthesis decrease skeletal density by consuming CO_2 and decreasing metabolic concentrations available for

$CaCO_3$ production (Swart et al. 2005). It is possible that variation in other environmental or physiological conditions impact both chromatophore and skeletal density independently. However, intra-site variation suggests against this and most environmental conditions were relatively consistent between sites. Extensive experimentation, such as controlled aquaria studies, are required to indicate direct causation between increased chromatophore density and decreased skeletal density. Still, our data suggests that chromatophores likely play an important role in coral physiology extending past simply protecting from UV radiation.

Physiological response of O. annularis to human pollution and disease susceptibility

A variety of anthropogenic pollution sources have been correlated with an increase in the occurrence of many important coral diseases including: black band disease (Frias-Lopez et al. 2002; Kuta and Richardson 2002; Kaczmarsky et al. 2005; Voss and Richardson, 2006), aspergillosis (Kim and Harvell, 2002; Bruno et al. 2003), yellow band disease (Bruno et al. 2003), and white plague II (Kaczmarsky et al. 2005). Our results support the findings of previous studies (Walker and Ormand, 1982; Hayes and Goreau, 1998; Klaus et al. 2007) that human sewage pollution weakens the coral holobiont and alters the physiology of the *O. annularis*. Zooxanthellae tissue cell density was negatively impacted by exposure to pollution with significantly higher tissue density measured at Jan Thiel (the pristine locale) than at sites downstream from the source, with the lowest tissue density recorded at WP. An observed decrease in the total density of zooxanthellae within coral tissues causes the coral to compensate by increasing active heterotrophic feeding. This would have no impact on inorganic nutrient intake, because active feeding is the only source of Nitrogen and Phosphorous (Grottoli et al. 2006; Houlbrèque and Ferrier-Pagès, 2009), but sugar production via zooxanthellae photosynthesis is a crucial energy

source for *O. annularis* (Davies et al. 1977; Swart, 1983, Swart et al. 2005). Therefore, maintaining decreased zooxanthellae tissue densities would reduce total energy available to the colony. With less total available energy, the coral animal would have to alter its energy budget. Because our results indicate there is no change in chromatophore density or skeletal density, it is likely not reducing energy used for maintaining these structures. If *O. annularis* prioritizes energy use on maintenance of body and structure before immune function, this could explain the general increase in disease susceptibility.

Increased SST and coral bleaching have been associated with a weakening of the coral holobiont and an increase in disease susceptibility as well (Harvell et al. 1999; Rosenberg and Ben-Haim, 2002; Jones et al. 2004). When exposed to increased SST *O. annularis* has previously been shown to exhibit a similar response of zooxanthellae loss (Goreau and Macfarlane, 1990; McWilliams et al, 2005), which is visible under extreme conditions as coral bleaching. Though colonies sampled in high levels of pollution did not exhibit bleaching with zooxanthellae loss, these colonies maintain diminished populations compared with their pristine counterpart. Zooxanthellae loss visible during bleaching events occurs for brief periods of high SST (Hoegh-Guldberg, 1999; Berkelmans et al. 2004). Though the environmental stressors and mechanisms for zooxanthellae loss are different in both instances, we propose the diminished zooxanthellae tissue density is the common factor leading to a weakened holobiont and increased disease susceptibility. With decreased zooxanthellae tissue density, there is a decrease in total sugar available to the coral and consistency of available energy. In both cases, this will stress the colony and alter energy use by the organism (Porter et al. 1989; Grottoli et al. 2004). A decrease in immune system maintenance has been previously associated with coral bleaching (Palmer et al. 2010; Mydlarz et al. 2009; 2010). Mydlarz et al. (2009) suggests that the increase in disease susceptibility during

bleaching events is due to suppressed immune activity, represented by altered activity of prophenoloxidase (PPO), peroxidase (POX), lysozyme-like (LYS) and antibacterial (AB) activity. We hypothesize a similar response in colonies exposed to anthropogenic pollution. This has been previously suggested by Hayes and Goreau (1998). They hypothesized increased disease prevalence may be due to a decrease in coral defense such as mucus production, nematocysts, mesenterial filaments and cilia. It is likely that a similar physiological response is occurring in organisms exposed to pollution.

To test this, future studies needs to be done quantifying the impacts of zooxanthellae loss in apparently unbleached colonies. Though the physiological importance of zooxanthellae are well-established and it is clear energy loss is significant in bleaching events, little has been done to look at the impacts of zooxanthellae loss in apparently unbleached corals. Quantifying this would give insight on the overall impacts of decreased zooxanthellae concentration on the metabolism of *O. annularis.* The immune activity of corals should be studied with zooxanthellae density along a polluted coast. Evaluating immune system activity, by quantifying mucocyte density and activity, nematocyst density, PPO, POX, LYS, or AB, is important for understanding the direct impacts of zooxanthellae loss on coral energy budgeting.

Chapter Six

Conclusions

Exposure to human sewage pollution significantly decreases zooxanthellae tissue cell density of *O. annularis.* This decrease in zooxanthellae tissue cell density in corals exposed to human sewage pollution encourages a shift to heterotrophy, weakens the coral holobiont and over time increases susceptibility to disease. A decrease in chromatophore tissue density was expected as well, however there was no significant positive correlation with concentration of human sewage pollution. Instead, significantly greater concentrations were observed in colonies from Snake Bay, and significant variation was seen between the polyps from different colonies at the same locale. This suggests variables associated with colony phenotype are more likely to impact chromatophore density than environmental factors. Furthermore, skeletal density did not have a significant relationship with pollution and there was no significant variation between any of the locales. This may be due to small sample size, or large intra-site variation in skeletal density. Because abiotic conditions were constant within each locale, this suggests biotic factors, such as metabolic CO_2 availability, may influence skeletal density.

Future studies, trying to understand the impacts of human sewage pollution on the coral holobiont and disease susceptibility should look at more coral cellular components known to be related to environmental stress such as mucocyte density, and carbonic anhydrase abundance. This may help create a better understanding of how anthropogenic pollution impacts weakens the coral holobiont and increases risk of disease. Additionally, more controlled aquaria studies on fragments from the same colony are necessary for limiting the impacts of environmental and genotypic variation.

Chapter Seven

Figures and Tables

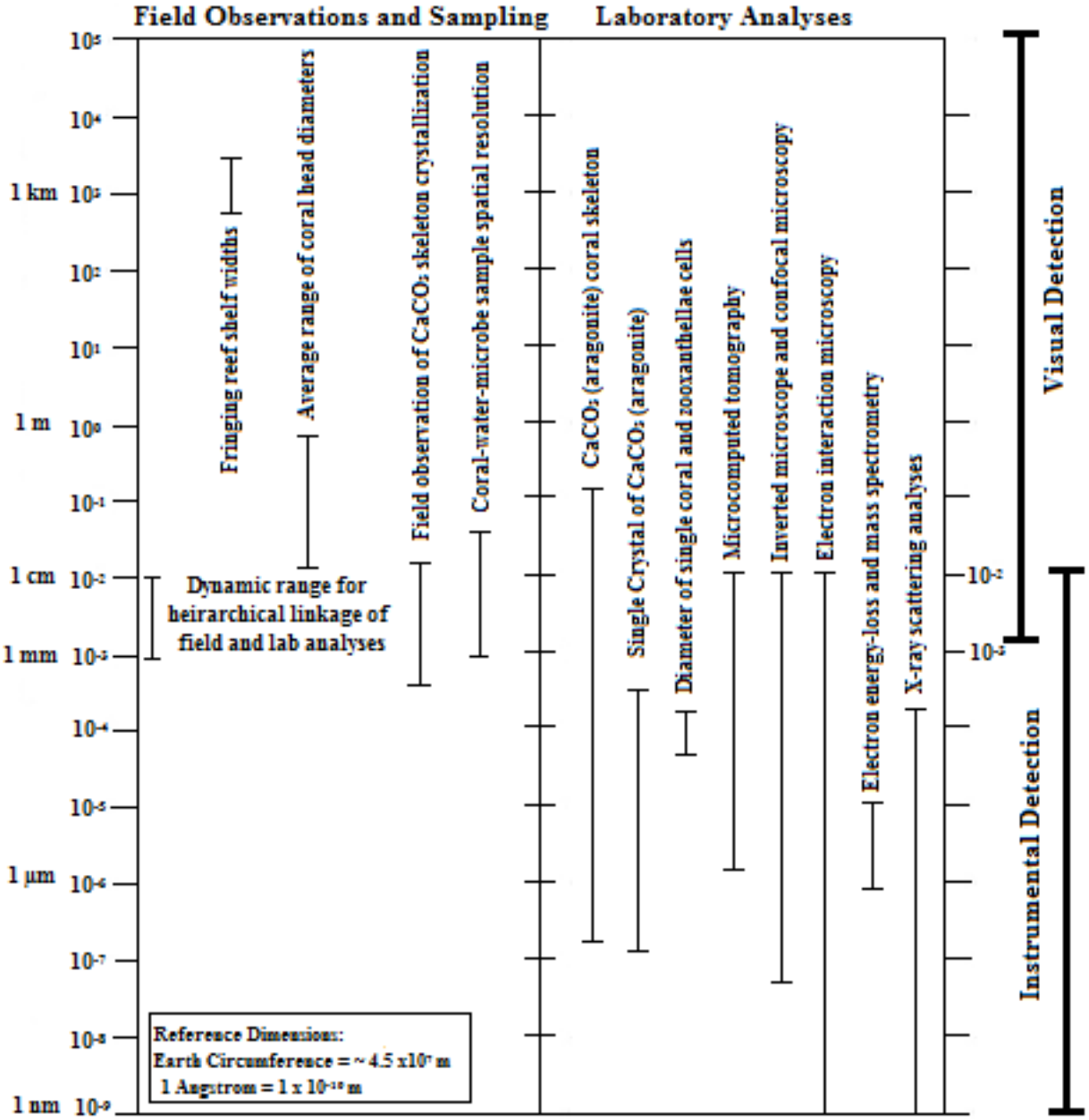

Figure 1. The 'Powers of Ten' hierarchal spatial scale for studying coral reef ecosystems (Modified from Sivaguru et al. 2014).

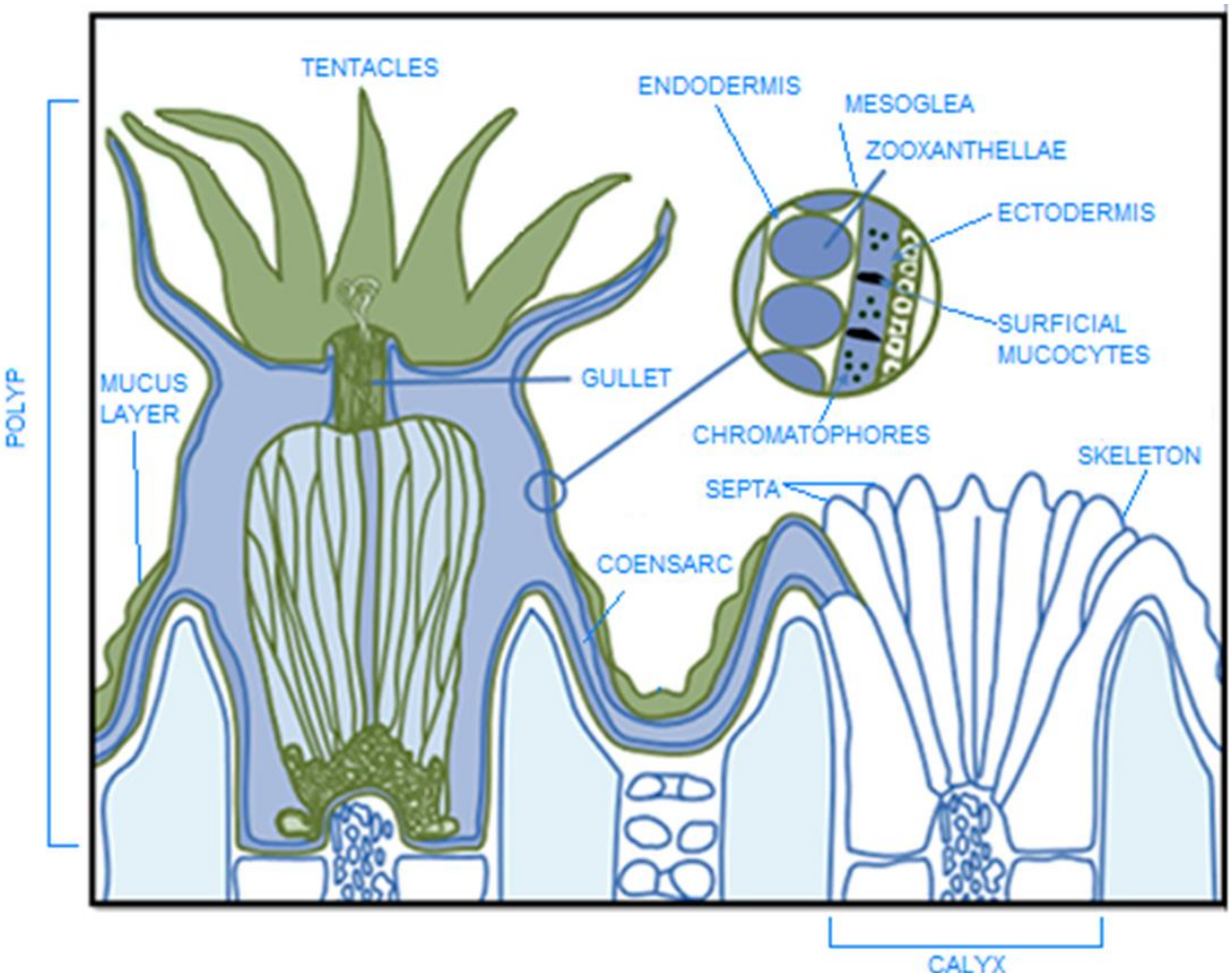

Figure 2. Cross-section model of the coral holobiont (Modified from Buddemeier et al. 2004)

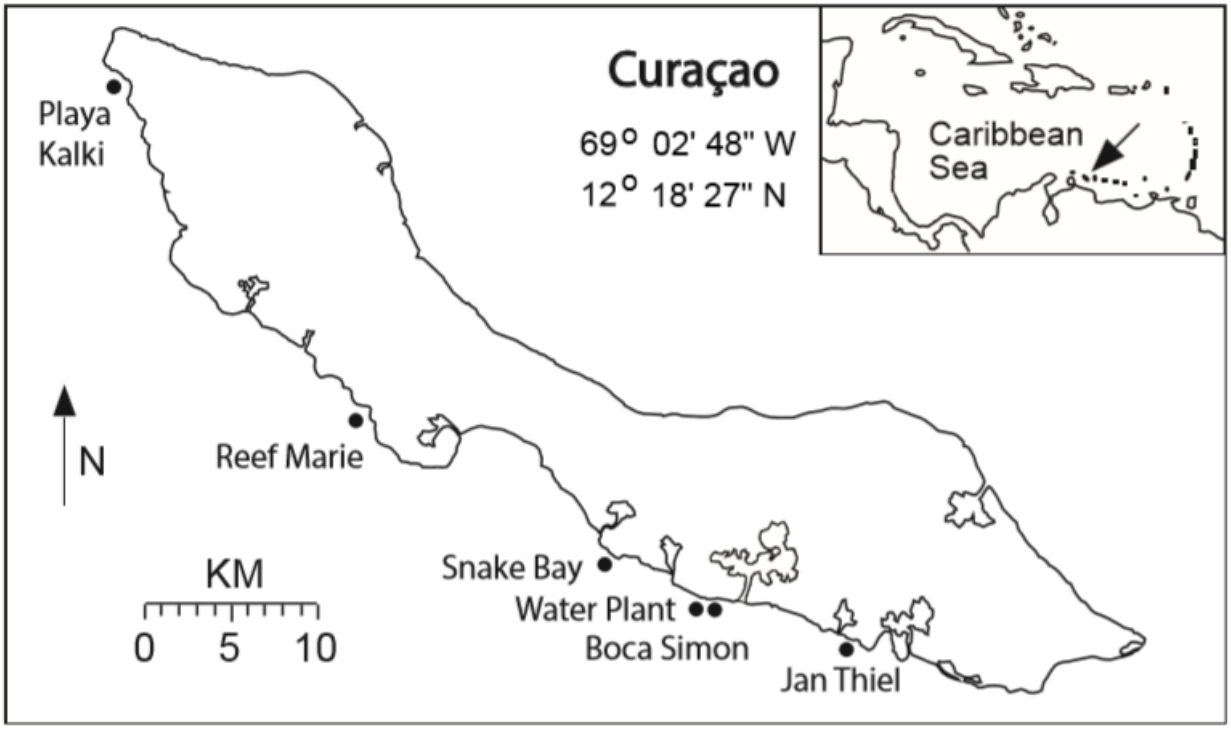

Figure 3. Map of Curacao. The five sites sampled for this study are shown on the map along with their proximity to the point source of anthropogenic pollution. The unidirectional moving from SE to NW is shown as well (Modified from Klaus et al 2005).

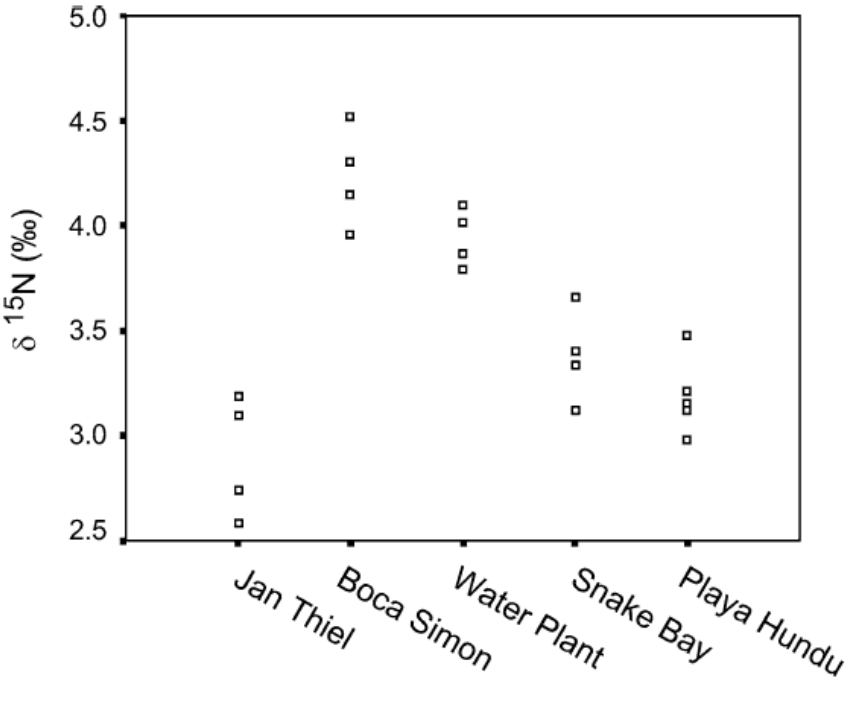

Figure 4. Tissue $\delta^{15}N$ of *O. annularis* colonies sampled at five sites along a gradient in human sewage pollution (Klaus et al. 2005).

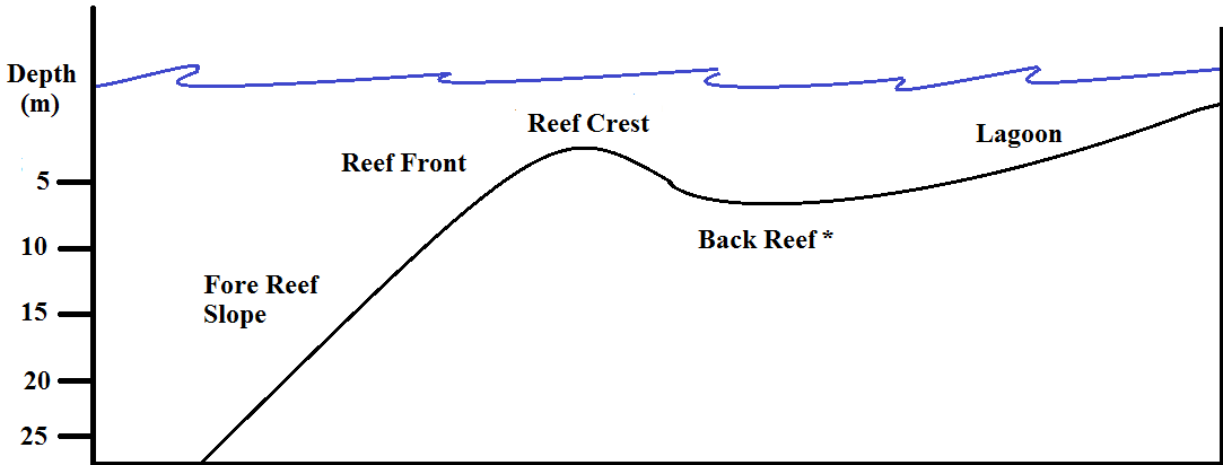

Figure 5. Reef facies model based off work of Wilson, 1974; James, 1978; Flugel, 1981.

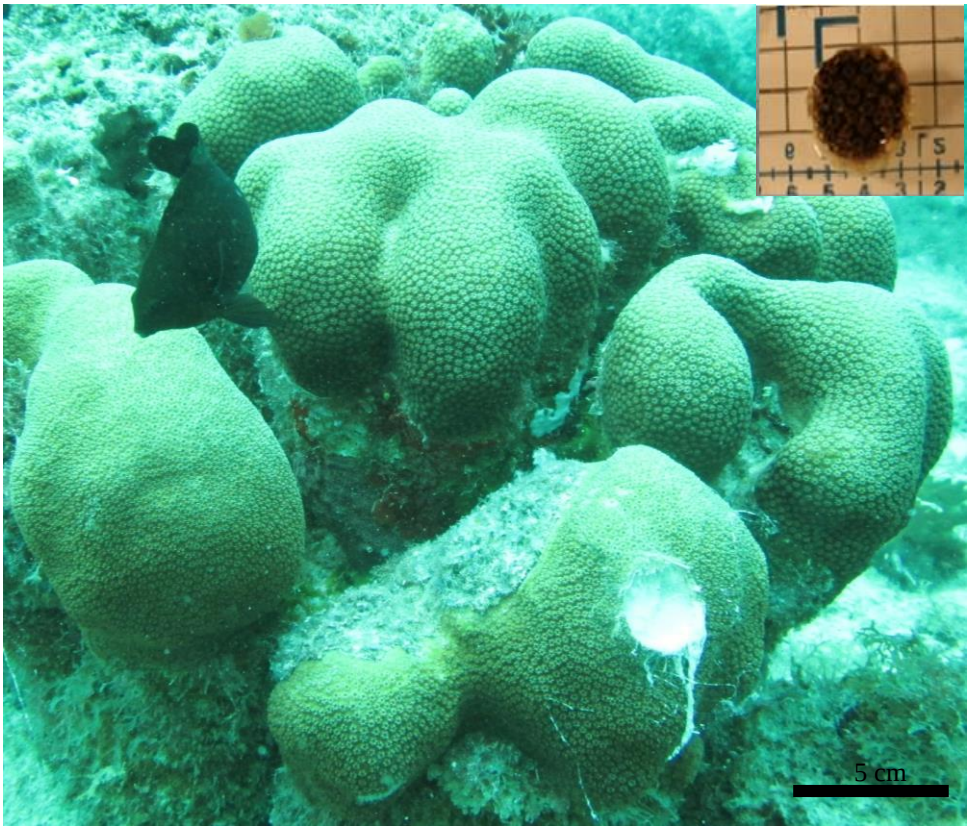

Figure 6. *O. annularis* colony with one tissue-skeletal biopsy removed.

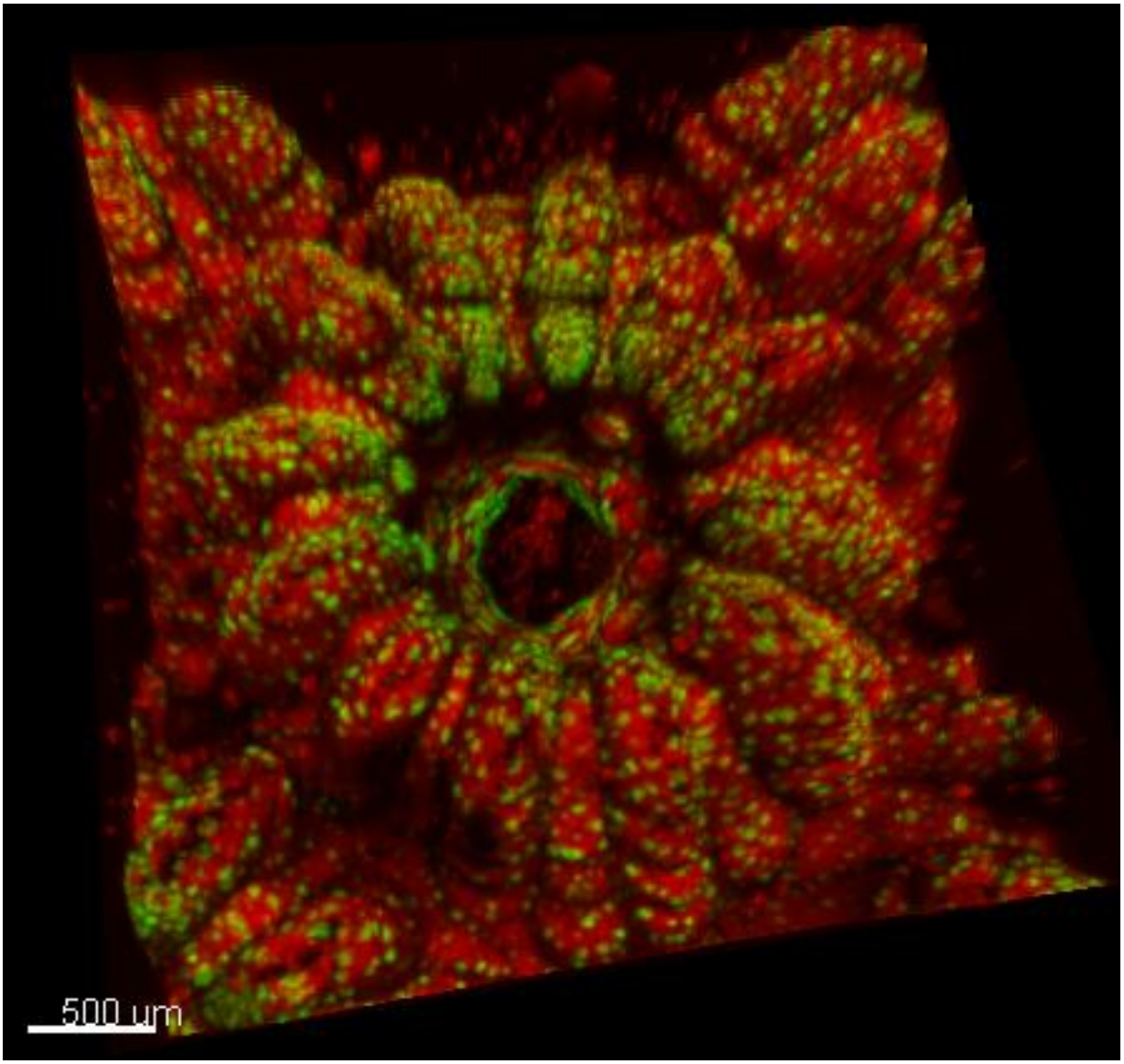

Figure 7. IMARIS 3D reconstruction of LSM 710 image of *O. annularis* polyp.

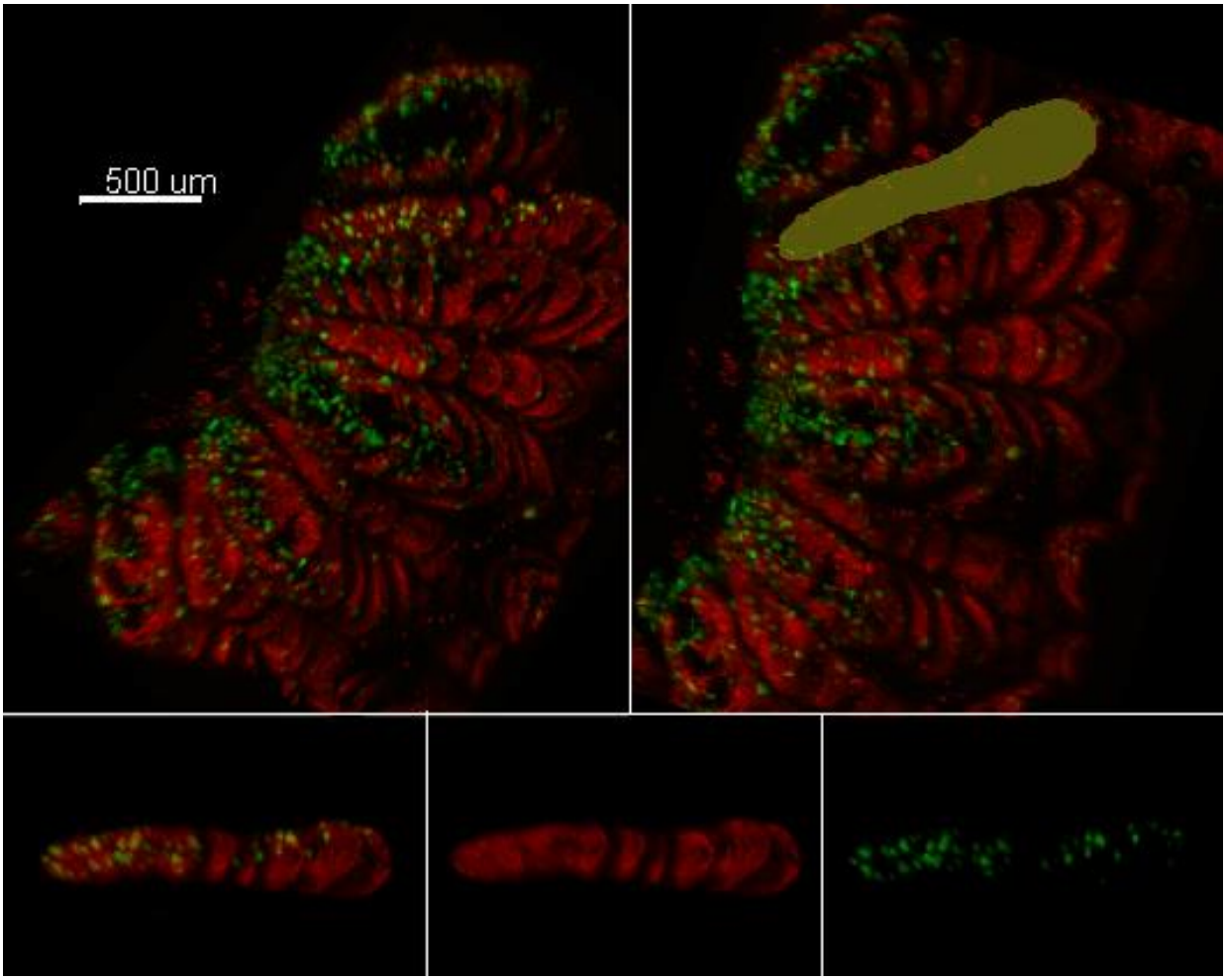

Figure 8. A) IMARIS 3D recreation of half polyp imaged with LSM 710 B) Secondary septa tissue isolated from half polyp C) Isolated secondary septa used for analysis D) Zooxanthellae cells of isolated secondary septa E) Chromatophore cells of isolated secondary septa

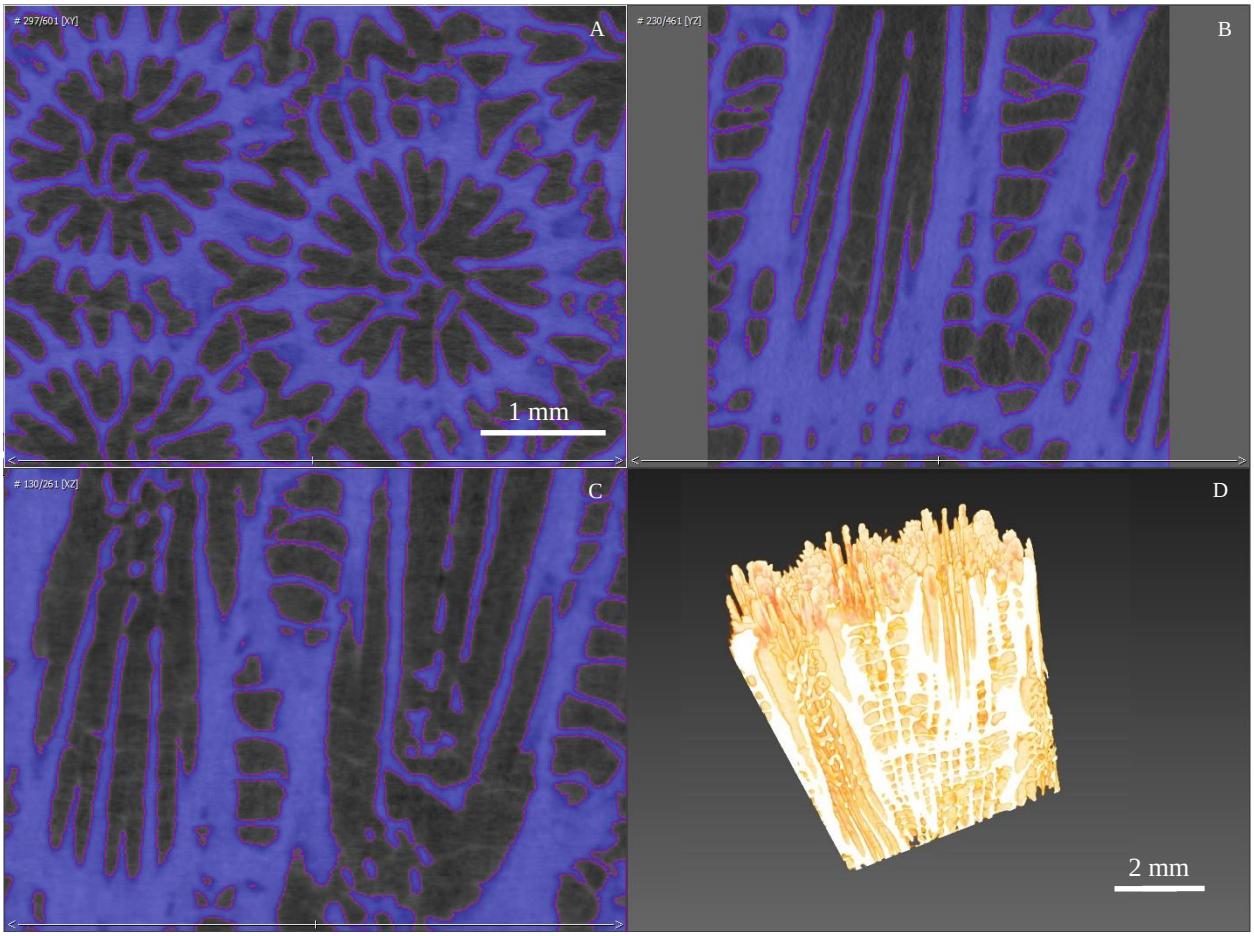

Figure 9. A) XY plane with thresholding of skeleton in AMIRA B) YZ plane with thresholding of skeleton C) XZ plane with thresholding of skeleton D) AMIRA 3D reconstruction of skeletal thick section using thresholding technique.

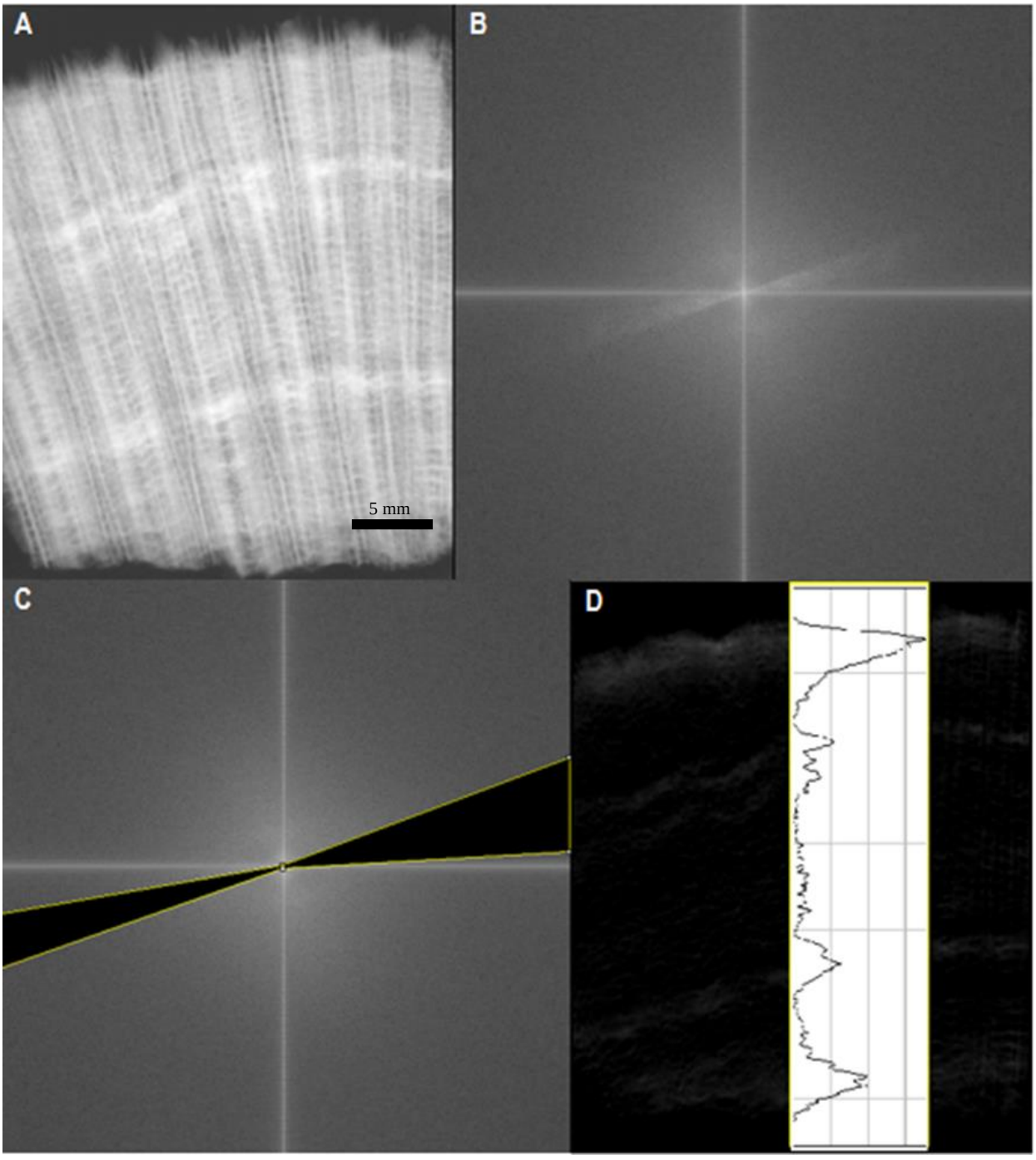

Figure 10. A) 2D unaltered BioCT scan of skeleton B) Fast-Fourier Transformation (FFT) plot of 2D skeletal image C) Altered FFT plot with vertical banding removed D) Inverse FFT plot of skeletal image with gray scale plot of averaged gray-scale values overlying.

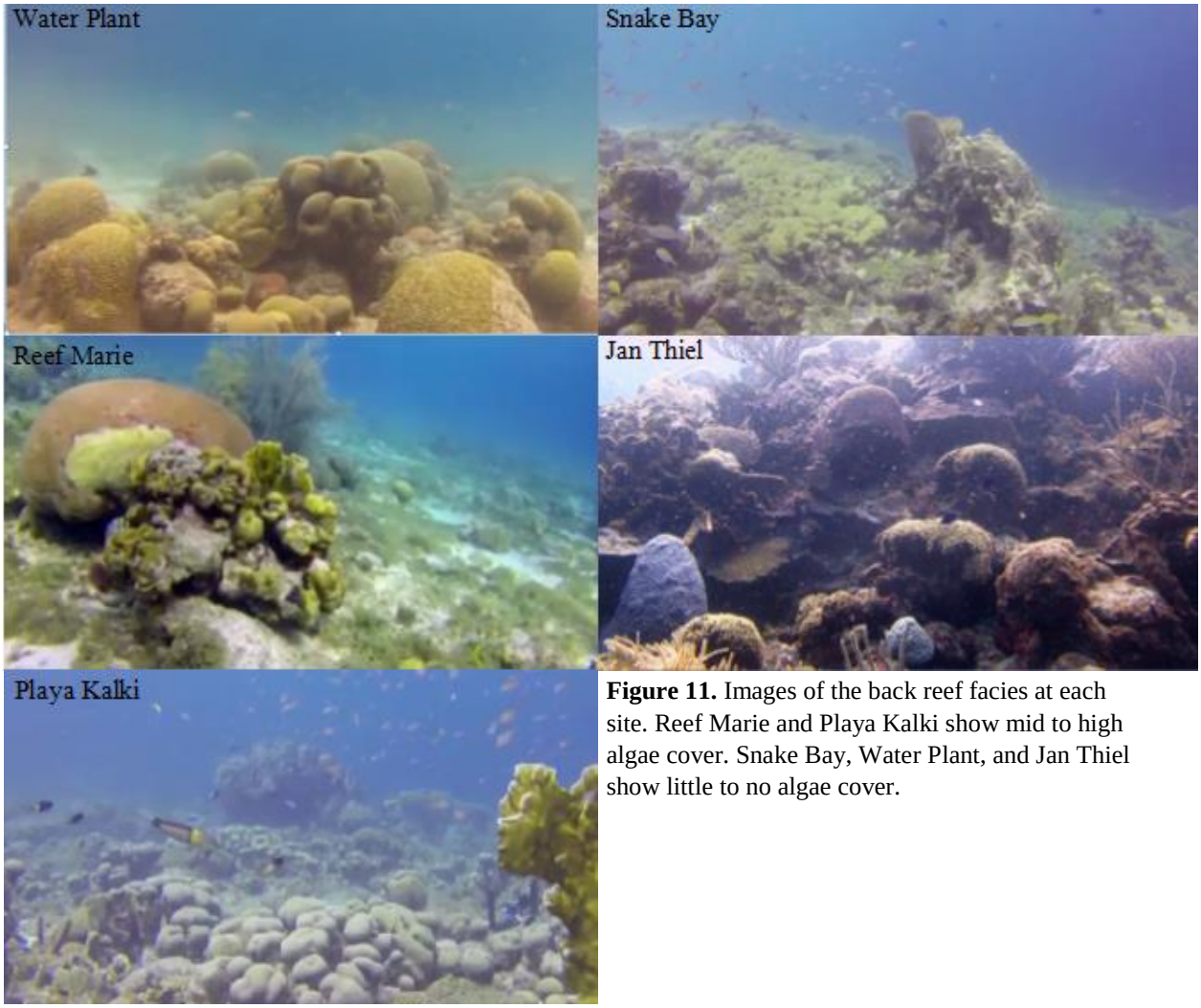

Figure 11. Images of the back reef facies at each site. Reef Marie and Playa Kalki show mid to high algae cover. Snake Bay, Water Plant, and Jan Thiel show little to no algae cover.

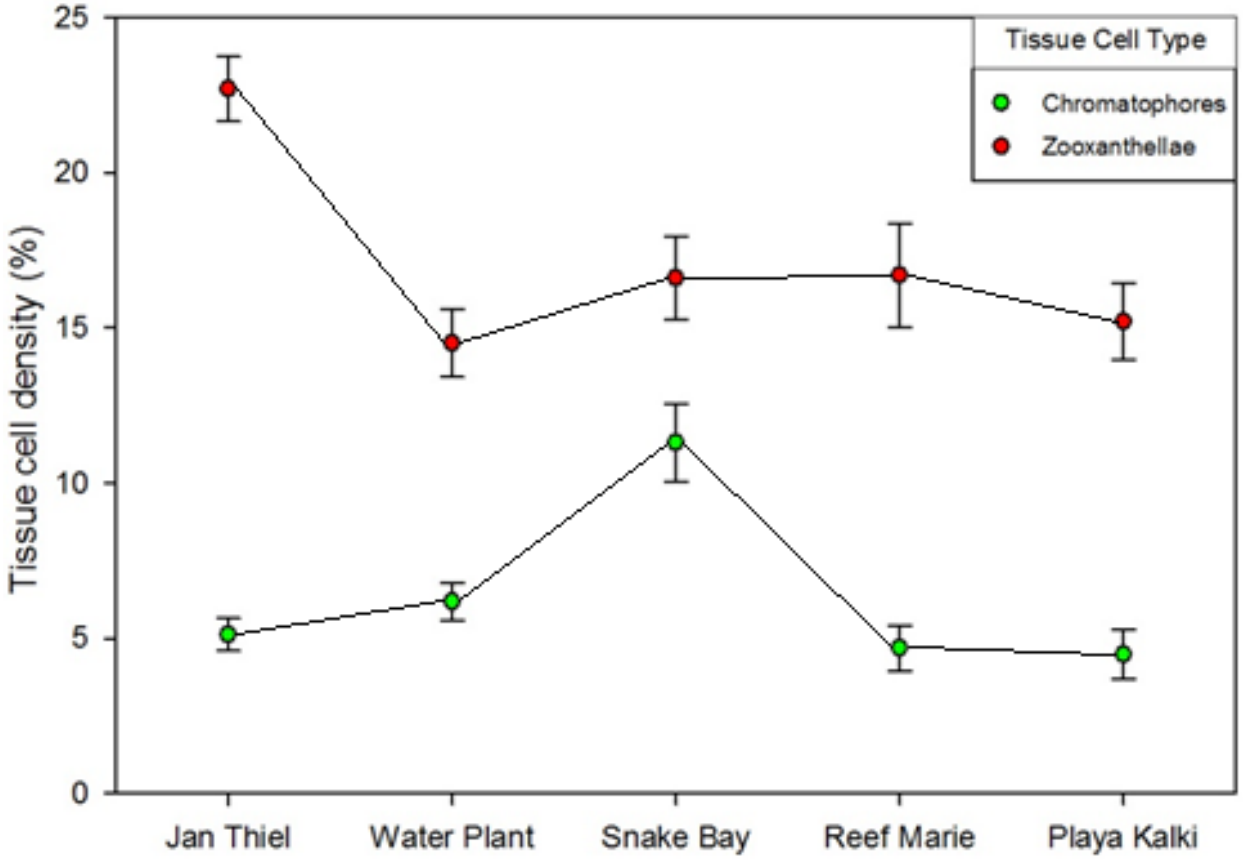

Figure 12. Average zooxanthellae and chromatophore tissue cell densities of three *O. annularis* colonies sampled at five locales along the southern coast of Curacao.

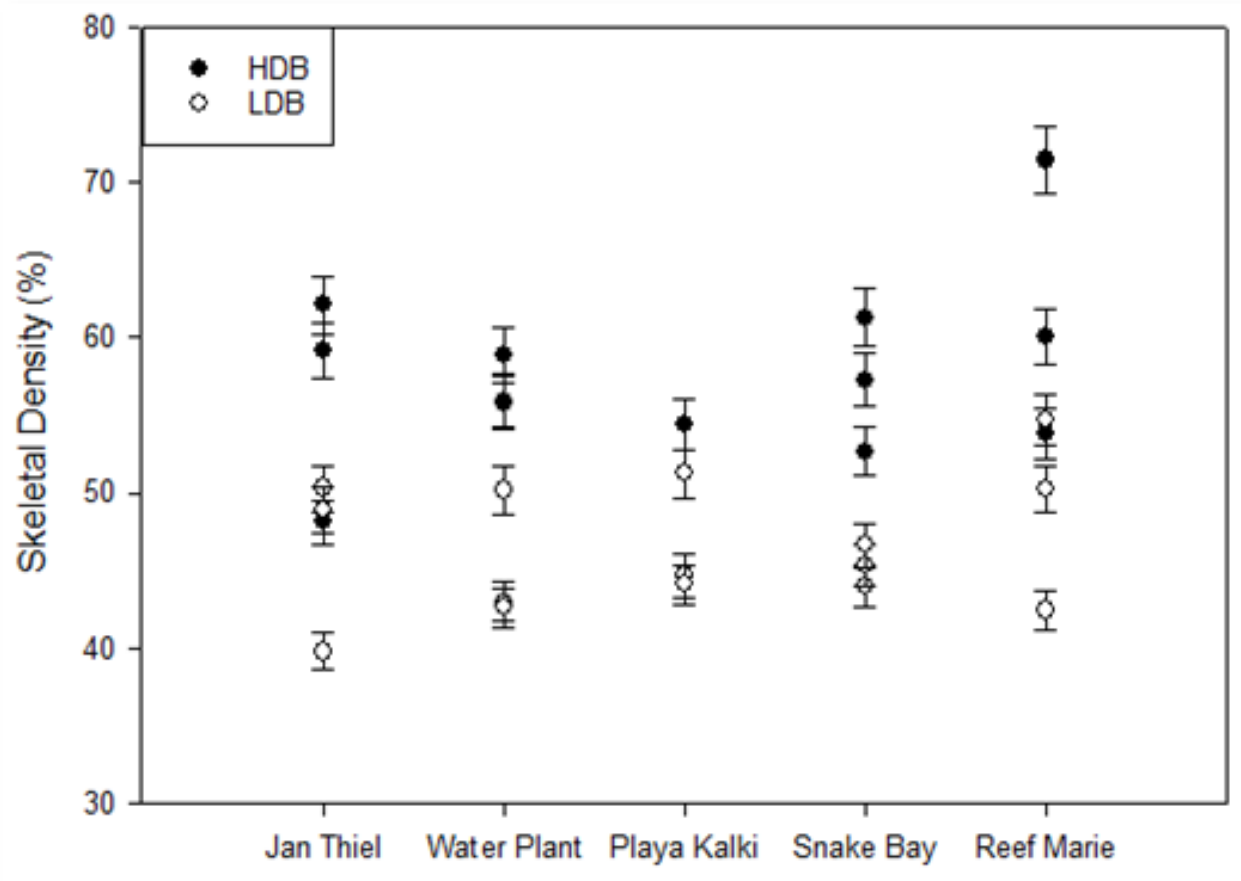

Figure 13. Average density (%) of High Density Band (HDB) and Low Density Band (LDB) of three colonies sampled at five locales along the southern coast of Curacao.

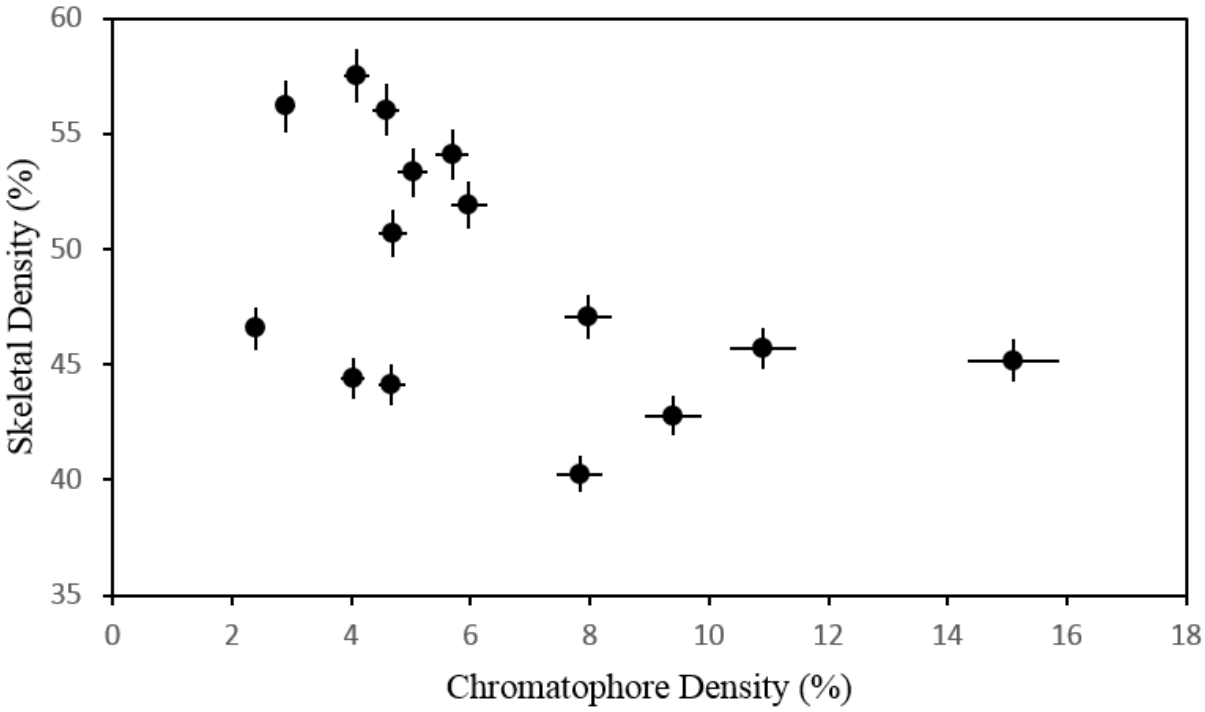

Figure 14. Linear correlation comparing chromatophore tissue cell density and skeletal density at the growing surface (top 0.5 mm) for each colony sampled.

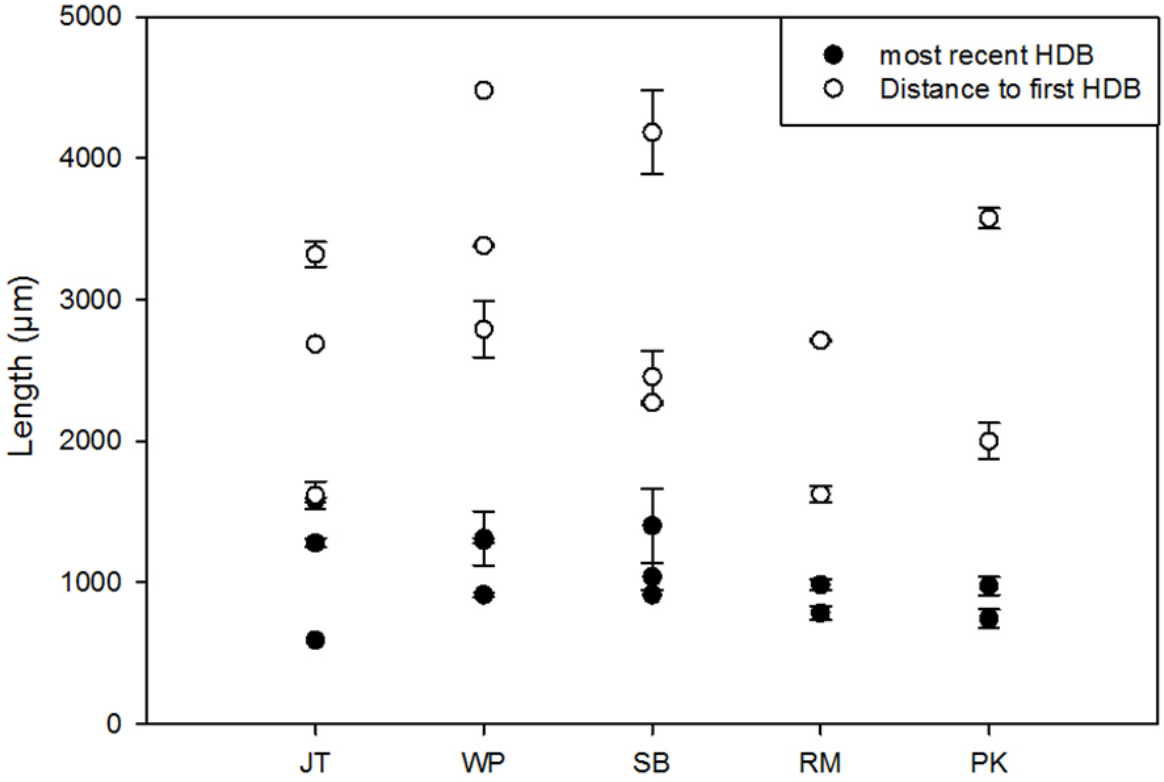

Figure 15. Average HDB width and distance to first HDB from the growing surface for three colonies sampled at the five locales along Curacao's southern coast.

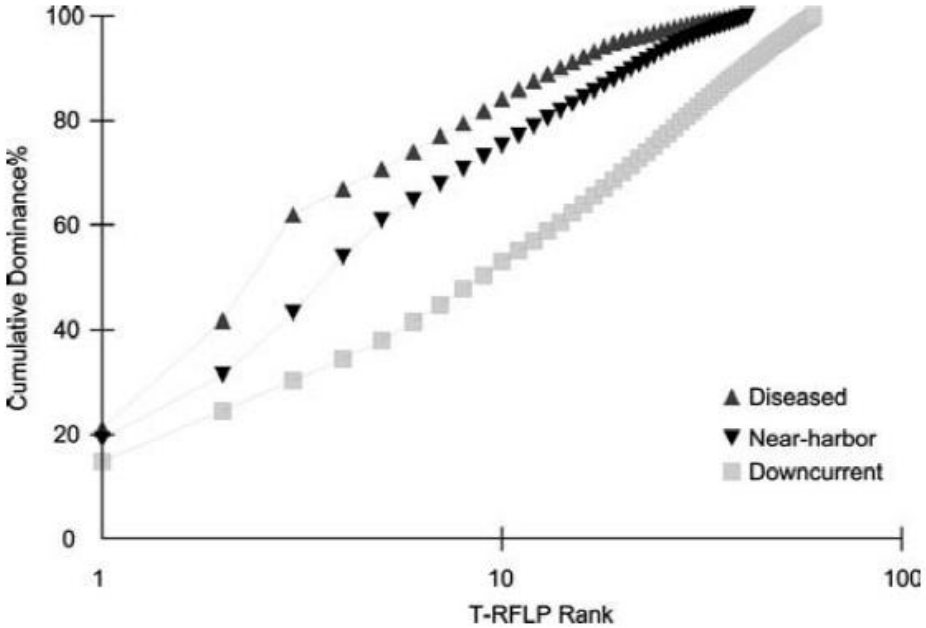

Figure 16. Average k-dominace curve of T-RFLP rank for diseased colonies and "apparently healthy" colonies sampled near– harbor pollution, and down-current from pollution source (Klaus et al. 2005).

Table 1. Temperature, water depth and photosynthetic active radiation at time of sampling for each colony.

Sampled Colony	Temperature (°C)	Depth (m)	PAR (%)
JT1	**26**	**7.7**	**24.98**
JT2	**26**	**8.3**	**19.56**
JT3	**26**	**7.6**	**15.47**
WP1	**26**	**7.7**	**104.16**
WP2	**26**	**6.1**	**71.19**
WP3	**26**	**7.3**	**74.08**
SB1	**26**	**7.0**	**22.92**
SB2	**26**	**5.9**	**32.10**
SB3	**26**	**6.1**	**----**
RM1	**26**	**7.1**	**72.78**
RM2	**26**	**6.1**	**91.85**
RM3	**26**	**6.4**	**24.10**
PK1	**26**	**6.4**	**15.99**
PK2	**26**	**6.6**	**37.07**
PK3	**26**	**6.8**	**----**

Table 2. Zooxanthellae, chromatophore, and skeletal total tissue volume and percent zooxanthellae and chromatophore density for each analyzed secondary septa.

Colony	Polyp	Zooxanthellae Vol. (um^3)	Chromatophore Vol. (um^3)	Total Tissue Vol. (um^3)	% Zoox.	% Chrom.
JT1	1	5.32E+06	1.43E+06	1.68E+07	31.7	8.50
	2	3.20E+06	3.20E+05	1.41E+07	22.7	2.27
		5.16E+06	4.96E+05	2.14E+07	24.1	2.32
		9.61E+05	2.11E+05	2.86E+06	33.6	7.39
		4.17E+06	5.07E+05	2.09E+07	20.0	2.43
JT2	1	1.75E+06	2.09E+05	8.60E+06	20.4	2.43
	2	1.04E+06	5.22E+04	3.67E+06	28.3	1.42
		9.49E+05	9.16E+04	3.23E+06	29.4	2.84
	3	1.52E+06	2.99E+05	1.93E+07	7.86	1.55
		7.93E+05	1.84E+05	2.92E+06	27.2	6.31
JT3	1	2.04E+06	7.61E+05	9.44E+06	21.6	8.06
		8.19E+05	3.43E+05	4.38E+06	18.7	7.84
	2	6.34E+05	2.62E+05	2.88E+06	22.0	9.11
		1.53E+06	7.75E+05	9.58E+06	16.0	8.09
		1.53E+06	5.47E+05	9.06E+06	16.9	6.04

Table 2. continued

PK1	1	3.57E+06	7.08E+05	3.15E+07	11.3	2.25
		4.67E+06	1.38E+06	2.16E+07	21.6	6.38
		1.26E+06	2.17E+05	6.74E+06	18.7	3.21
	2	1.22E+06	4.35E+05	8.67E+06	14.1	5.02
		1.77E+06	5.05E+05	7.61E+06	23.3	6.63
PK2	1	2.28E+06	1.08E+06	2.09E+07	10.9	5.47
		1.65E+06	2.75E+05	1.64E+07	10.1	4.06
	2	2.09E+06	5.05E+05	1.35E+07	15.5	3.74
		3.54E+06	9.66E+05	2.38E+07	14.9	1.68
		6.07E+06	1.77E+06	3.24E+07	18.7	5.19
PK3	1	3.37E+06	1.76E+06	1.77E+07	19.0	9.95
		1.44E+06	2.38E+05	1.02E+07	14.1	2.33
	2	3.28E+06	9.13E+05	2.36E+07	13.9	3.87
		1.22E+06	4.53E+05	1.10E+07	11.1	4.12
	3	2.89E+06	8.24E+05	2.61E+07	11.1	3.16
RM1	1	3.47E+06	2.97E+05	1.83E+07	19.0	1.62
		5.81E+06	6.57E+05	2.81E+07	20.7	2.34
		4.30E+06	7.59E+05	2.50E+07	17.2	3.04
	2	3.38E+06	5.06E+05	2.07E+07	16.3	2.45
	3	4.89E+06	7.44E+05	2.92E+07	16.7	2.55
RM2	1	1.36E+06	3.79E+05	8.22E+06	16.5	4.61
	2	3.14E+06	1.08E+06	1.76E+07	17.9	6.14
		5.38E+05	2.47E+05	5.10E+06	10.5	4.84
	3	4.08E+06	2.54E+06	4.24E+07	9.61	6.00
		2.74E+06	8.10E+05	1.18E+07	23.2	6.86
RM3	1	2.11E+06	7.80E+05	9.60E+06	22.0	8.13
		1.45E+06	7.35E+05	1.13E+07	12.9	6.51
		1.09E+06	5.20E+05	1.05E+07	10.4	4.95
	2	2.14E+06	1.23E+06	1.35E+07	15.9	9.13
	3	4.92E+06	2.50E+05	2.21E+07	22.3	1.13
SB1	1	1.69E+06	1.18E+06	7.92E+06	21.3	14.9
	2	6.50E+06	4.23E+06	3.31E+07	19.6	12.8
		5.27E+06	2.97E+06	2.91E+07	18.1	10.2
	3	4.73E+06	2.11E+06	3.02E+07	15.7	6.97
		5.45E+06	2.70E+06	2.80E+07	19.5	9.64

Table 3. Average % Zooxanthellae and Chromatophore per total secondary septa tissue volume at each colony and at each site.

Site	Colony	Average % Zoox.	Standard Error % Zoox.	Average % Chrom	Standard Error % Chrom
JT	1	26.4	2.37	4.58	1.24
	2	22.6	3.59	2.91	0.796
	3	19.0	1.08	7.83	0.446
	Combined	22.7	1.67	5.11	0.736
PK	1	17.8	2.01	4.70	0.771
	2	14.0	1.42	4.03	0.601
	3	13.8	1.30	4.68	1.21
	Combined	15.2	1.04	4.47	0.525
RM	1	18.0	0.722	2.40	0.204
	2	15.6	2.24	5.69	0.378
	3	16.7	2.14	5.97	1.25
	Combined	16.7	1.05	4.68	0.941
SB	1	18.8	0.844	10.9	1.22
	2	14.5	3.31	15.1	1.57
	3	16.6	1.69	7.97	2.26
	Combined	16.6	1.35	11.3	1.25
WP	1	15.8	1.34	9.40	1.00
	2	16.5	2.42	4.09	0.628
	3	11.2	1.65	5.03	0.940
	Combined	14.5	1.23	6.17	0.781

Table 4. P-values comparing percent zooxanthellae tissue density of the five different locales (bolded if statistically significant, $P<0.05$).

Site	JT	PK	RM	SB	WP
JT	---	**3.16E-03**	**8.12E-03**	**1.63E-02**	**7.48E-04**
PK	---	---	0.292	0.378	0.676
RM	---	---	---	0.957	0.263
SB	---	---	---	---	0.325
WP	---	---	---	---	---

Table 5. P-values comparing percent chromatophore tissue density of the five different locales (bolded if statistically significant, P<0.05).

Site	JT	PK	RM	SB	WP
JT	---	0.536	0.642	**3.93E-03**	0.405
PK	---	---	0.787	**4.42E-04**	0.0756
RM	---	---	---	**3.22E-04**	0.286
SB	---	---	---	---	**3.15E-03**
WP	---	---	---	---	---

Table 6. Percent density of high density Band (HDB) closest to growing surface

Sample	% HDB Density	Site Average	Site STE
JT1	72.72		
JT2	66.43		
JT3	62.39	67.18	2.453981
WP1	69.96		
WP2	75.95		
WP3	58.53	68.14666667	7.226351
PK1	----		
PK2	----		
PK3	69.19	----	----
SB1	----		
SB2	66.24		
SB3	66.6	----	----
RM1	74.85		
RM2	77.53		
RM3	71.54	74.64	1.414457

Table 7. Percent density of low density band (LDB) deposited before measured HDB

Sample	% LDB Density	Site Average	Site STE
JT1	59.61		
JT2	55.15		
JT3	49.47	54.74333333	2.39578
WP1	60.58		
WP2	60.81		
WP3	51.76	57.71666667	2.432403
PK1	51.24		
PK2	52.35		
PK3	62.42	55.33666667	2.90357
SB1	55.48		
SB2	56.09		
SB3	57.33	56.3	0.444397
RM1	62.03		
RM2	62.44		
RM3	65.88	63.45	0.996739

Table 8. Width of most recently deposited HDB for each colony at all five locales.

Colony	HDB width one (µm)	HDB width two (µm)	Mean HDB width per colony (µm)	STD HDB width per colony (µm)	Mean HDB width per site (µm)
JT1	1248	1312	1280	32	1152
JT2	592		592		
JT3	1568	1600	1584	16	
WP1	1504	1120	1312	192	1173.33
WP2	928	896	912	16	
WP3	1280	1312	1296	16	
SB1	912	912	912	0	1117.33
SB2	1664	1136	1400	264	
SB3	1136	944	1040	96	
RM1	832	736	784	48	884
RM2	1024	944	984	40	
RM3					
PK1					860
PK2	800	672	744	64	
PK3	912	1040	976	64	

Table 9. Average skeletal density for the growing surface (top 0.5 mm) of each sampled colony.

Sample	Growing surface density (%)
JT1	56.05
JT2	56.2
JT3	40.25
WP1	42.77
WP2	57.54
WP3	53.34
PK1	50.71
PK2	44.43
PK3	44.13
SB1	45.71
SB2	45.18
SB3	47.06
RM1	46.58
RM2	54.13
RM3	51.92

Chapter Eight

References

Al-Horani, F. A. (2005). Effects of changing seawater temperature on photosynthesis and calcification in the scleractinian coral Galaxea fascicularis, measured with O 2, Ca 2+ and pH microsensors. *Scientia Marina*, *69*(3), 347-354.

Al-Moghrabi, S. (2001). Unusual black band disease (BBD) outbreak in the northern tip of the Gulf of Aqaba (Jordan). *Coral Reefs*, *19*(4), 330-331.

Aronson, R. B., & Precht, W. F. (2001). White-band disease and the changing face of Caribbean coral reefs. In *The Ecology and Etiology of Newly Emerging Marine Diseases* (pp. 25-38). Springer Netherlands.

Bak, R. P., & Luckhurst, B. E. (1980). Constancy and change in coral reef habitats along depth gradients at Curacao. *Oecologia*, *47*(2), 145-155.

Bak, R. P. M., & Nieuwland, G. (1995). Long-term change in coral communities along depth gradients over leeward reefs in the Netherlands Antilles. *Bulletin of Marine Science*, *56*(2), 609-619.

Bak, R. P., Brouns, J. J. W. M., & Heys, F. M. L. (1977). Regeneration and aspects of spatial competition in the scleractinian corals Agaricia agaricites and Montastrea annularis. In *Proceedings of the 3rd International Coral Reef Symposium, Miami* (pp. 143-148).

Baker, D. M., MacAvoy, S. E., & Kim, K. (2007). Relationship between water quality, delta^ 1^ 5N, and aspergillosis of Caribbean sea fan corals. *MARINE ECOLOGY-PROGRESS SERIES-*, *343*, 123.

Ban, Stephen S., Nicholas AJ Graham, and Sean R. Connolly. "Evidence for multiple stressor interactions and effects on coral reefs." *Global change biology*20.3 (2014): 681-697.

Barnes, D. J., & Lough, J. M. (1993). On the nature and causes of density banding in massive coral skeletons. *Journal of Experimental Marine Biology and Ecology*, *167*(1), 91-108.

Bentis, C. J., Kaufman, L., & Golubic, S. (2000). Endolithic fungi in reef-building corals (Order: Scleractinia) are common, cosmopolitan, and potentially pathogenic.*Biological bulletin*, 254-260.

Berkelmans, R., De'ath, G., Kininmonth, S., & Skirving, W. J. (2004). A comparison of the 1998 and 2002 coral bleaching events on the Great Barrier Reef: spatial correlation, patterns, and predictions. *Coral reefs*, *23*(1), 74-83.

Brandt, M. E., & McManus, J. W. (2009). Disease incidence is related to bleaching extent in reef-building corals. *Ecology*, *90*(10), 2859-2867.

Brown, B. E. (1997). Coral bleaching: causes and consequences. *Coral reefs*,*16*(1), S129-S138.

Brown, B. E., & Bythell, J. C. (2005). Perspectives on mucus secretion in reef corals. *Marine Ecology Progress Series*, *296*, 291-309.

Brown, B. E., Le Tissier, M. D. A., & Bythell, J. C. (1995). Mechanisms of bleaching deduced from histological studies of reef corals sampled during a natural bleaching event. *Marine Biology*, *122*(4), 655-663.

Bruckner, A. W., & Bruckner, R. J. (2006). The recent decline of Montastraea annularis (complex) coral populations in western Curaçao: a cause for concern?.*Revista de Biología Tropical*, *54*, 45-58.

Bruno, J. F., Petes, L. E., Drew Harvell, C., & Hettinger, A. (2003). Nutrient enrichment can increase the severity of coral diseases. *Ecology letters*, *6*(12), 1056-1061.

Bruno, J. F., Selig, E. R., Casey, K. S., Page, C. A., Willis, B. L., Harvell, C. D., Sweatman H., & Melendy, A. M. (2007). Thermal stress and coral cover as drivers of coral disease outbreaks. *PLoS biology*, *5*(6), e124.

Budd, A. F., & Klaus, J. S. (2001). The origin and early evolution of the Montastraea "annularis" species complex (Anthozoa: Scleractinia). *Journal Information*, *75*(3).

Budd, A. F., Johnson, K. G., & Stemann, T. A. (1996). Plio-Pleistocene turnover and extinctions in the Caribbean reef coral fauna. *Evolution and environment in tropical America*, 168-204.

Budd, A. F., Fukami, H., Smith, N. D., & Knowlton, N. (2012). Taxonomic classification of the reef coral family Mussidae (Cnidaria: Anthozoa: Scleractinia).*Zoological Journal of the Linnean Society*, *166*(3), 465-529.

Buddemeier, R. W., & Fautin, D. G. (1993). Coral bleaching as an adaptive mechanism. *Bioscience*, 320-326.

Cao, L., Caldeira, K., & Jain, A. K. (2007). Effects of carbon dioxide and climate change on ocean acidification and carbonate mineral saturation. *Geophysical Research Letters*, *34*(5).

Carricart-Ganivet, J. P. (2004). Sea surface temperature and the growth of the West Atlantic reef-building coral Montastraea annularis. *Journal of Experimental Marine Biology and Ecology*, *302*(2), 249-260.

Carricart-Ganivet, J. P., & Barnes, D. J. (2007). Densitometry from digitized images of X-radiographs: Methodology for measurement of coral skeletal density.*Journal of Experimental Marine Biology and Ecology*, *344*(1), 67-72.

Carricart-Ganivet, J. P., Beltrán-Torres, A. U., Merino, M., & Ruiz-Zárate, M. A. (2000). Skeletal extension, density and calcification rate of the reef building coral Montastraea annularis (Ellis and Solander) in the Mexican Caribbean. *Bulletin of Marine Science*, *66*(1), 215-224.

Cervino, J. M., Hayes, R. L., Honovich, M., Goreau, T. J., Jones, S., & Rubec, P. J. (2003). Changes in zooxanthellae density, morphology, and mitotic index in hermatypic corals and anemones exposed to cyanide. *Marine Pollution Bulletin*,*46*(5), 573-586.

Chamberlain Jr, J. A. (1978). Mechanical properties of coral skeleton: compressive strength and its adaptive significance. *Paleobiology*, 419-435.

Cohen, A. L., & McConnaughey, T. A. (2003). Geochemical perspectives on coral mineralization. *Reviews in mineralogy and geochemistry*, *54*(1), 151-187.

Connell, J. H. (1978). Diversity in tropical rain forests and coral reefs. *Science*,*199*(4335), 1302-1310.

Constantz, B. R. (1986). Coral skeleton construction: a physiochemically dominated process. *Palaios*, 152-157.

Cooper, T. F., De'Ath, G., Fabricius, K. E., & Lough, J. M. (2008). Declining coral calcification in massive Porites in two nearshore regions of the northern Great Barrier Reef. *Global Change Biology*, *14*(3), 529-538.

Cuif, J. P., & Dauphin, Y. (1998). Microstructural and physico-chemical characterization of ‘centers of calcification’in septa of some Recent scleractinian corals. *Paläontologische Zeitschrift*, *72*(3-4), 257-269.

Daszak, P., Cunningham, A. A., & Hyatt, A. D. (2001). Anthropogenic environmental change and the emergence of infectious diseases in wildlife. *Acta tropica*, *78*(2), 103-116.

Davies, P. S. (1984). The role of zooxanthellae in the nutritional energy requirements of Pocillopora eydouxi. *Coral Reefs*, *2*(4), 181-186.

Davies, J. M., Dunne, R. P., & Brown, B. E. (1997). Coral bleaching and elevated sea-water temperature in Milne Bay Province, Papua New Guinea, 1996. *Marine and Freshwater Research*, *48*(6), 513-516.

De'ath, G., & Fabricius, K. (2010). Water quality as a regional driver of coral biodiversity and macroalgae on the Great Barrier Reef. *Ecological Applications*,*20*(3), 840-850.

Dodge, R. E., Szmant-Froelich, A., Garcia, R., Swart, P. K., Forester, A., & Leder, J. J. (1993). Skeletal structural basis of density banding in the reef coral Montastrea annularis.

Dove, S. G., Hoegh-Guldberg, O., & Ranganathan, S. (2001). Major colour patterns of reef-building corals are due to a family of GFP-like proteins. *Coral reefs*, *19*(3), 197-204.

Downs, C. A., Fauth, J. E., Halas, J. C., Dustan, P., Bemiss, J., & Woodley, C. M. (2002). Oxidative stress and seasonal coral bleaching. *Free Radical Biology and Medicine*, *33*(4), 533-543.

Duyl, F. C. V. (1985). Atlas of the living reefs of Curacao and Bonaire (Netherlands Antilles).

Edmunds, P. J., & Elahi, R. (2007). The demographics of a 15-year decline in cover of the Caribbean reef coral Montastraea annularis. *Ecological Monographs*, *77*(1), 3-18.

Environmental Protection Agency. *Biosolids: Targeted National Sewage Sludge Survey Report.* Privacy and Security Notice, 2012.

Fabricius, K. E. (2005). Effects of terrestrial runoff on the ecology of corals and coral reefs: review and synthesis. *Marine pollution bulletin*, *50*(2), 125-146.

Fouke, B. W. (2001). Depositional Facies and Aqueous-Solid Geochemistry of Travertine-Depositing Hot Springs (Angel Terrace, Mammoth Hot Springs, Yellowstone National Park, USA): Reply. *Journal of sedimentary research*, *71*(3), 497-500.

Fouke, B. W. (2011). Hot-spring Systems Geobiology: abiotic and biotic influences on travertine formation at Mammoth Hot Springs, Yellowstone National Park, USA. *Sedimentology*, *58*(1), 170-219.

Flügel, E. (1981). Paleoecology and facies of Upper Triassic reefs in the Northern Calcareous Alps.

Fischer, H. B., List, J. E., Koh, C. R., Imberger, J., & Brooks, N. H. (2013). *Mixing in inland and coastal waters*. Elsevier.

Franklin, D. J., Hoegh-Guldberg, O., Jones, R.J. & Berges , J. A. (2004). Cell death and degeneration in the symbiotic dinoflagellates of the coral Stylophora pistillata during bleaching. *Marine Ecology Progress Series*, 272, 117-130.

Frias-Lopez, J., Bonheyo, G. T., Jin, Q., & Fouke, B. W. (2003). Cyanobacteria associated with coral black band disease in Caribbean and Indo-Pacific reefs.*Applied and Environmental Microbiology*, *69*(4), 2409-2413.

Frias-Lopez, J., Klaus, J. S., Bonheyo, G. T., & Fouke, B. W. (2004). Bacterial community associated with black band disease in corals. *Applied and Environmental Microbiology*, *70*(10), 5955-5962.

Frias-Lopez, J., Zerkle, A. L., Bonheyo, G. T., & Fouke, B. W. (2002). Partitioning of bacterial communities between seawater and healthy, black band diseased, and dead coral surfaces. *Applied and Environmental Microbiology*, *68*(5), 2214-2228.

Gast, G. J. (1998). Nutrient pollution in coral reef waters. In *Reef Care Curacao Workshop Nutr Pollut* (Vol. 5, p. 13).

Gattuso, J. P., Allemand, D., & Frankignoulle, M. (1999). Photosynthesis and calcification at cellular, organismal and community levels in coral reefs: a review on interactions and control by carbonate chemistry. *American Zoologist*, *39*(1), 160-183.

Gladfelter, E. H. (1983). Skeletal development inAcropora cervicornis. *Coral Reefs*, *2*(2), 91-100.

Goh, B. P. L., & Chou, L. M. (1997). Effects of the heavy metals copper and zinc on zooxanthellae cells in culture. *Environmental monitoring and assessment*,*44*(1-3), 11-19.

Goreau T. J., Hayes R. L. (1994) Coral bleaching and ocean 'hot spots'. Ambio, 23, 176-180.

Goreau, T. J., & Macfarlane, A. H. (1990). Reduced growth rate of Montastrea annularis following the 1987–1988 coral-bleaching event. *Coral Reefs*, *8*(4), 211-215.

Grottoli, A. G., Rodrigues, L. J., & Juarez, C. (2004). Lipids and stable carbon isotopes in two species of Hawaiian corals, Porites compressa and Montipora verrucosa, following a bleaching event. *Marine Biology*, *145*(3), 621-631.

Grottoli, A. G., Rodrigues, L. J., & Palardy, J. E. (2006). Heterotrophic plasticity and resilience in bleached corals. *Nature*, *440*(7088), 1186-1189.

Hallock, P. (2001). Coral reefs, carbonate sediments, nutrients, and global change. In *The history and sedimentology of ancient reef systems* (pp. 387-427). Springer US.

Harvell, C. D., Mitchell, C. E., Ward, J. R., Altizer, S., Dobson, A. P., Ostfeld, R. S., & Samuel, M. D. (2002). Climate warming and disease risks for terrestrial and marine biota. *Science*, *296*(5576), 2158-2162.

Harvell, D., Jordán-Dahlgren, E., Merkel, S., Rosenberg, E., Raymundo, L., Smith, G., Weil, E., & Willis, B. (2007). Coral disease, environmental drivers, and the balance between coral and microbial associates. *Oceanography*, *20*, 172-195.

Harvell, C. D., Kim, K., Burkholder, J. M., Colwell, R. R., Epstein, P. R., Grimes, D. J., Hofmann, E. E., Lipp, E. K., Osterhaus, A. D. M. E., Overstreet, R. M., Porter, J. W., Smith, G. W., & Vasta, G. R. (1999). Emerging marine diseases--climate links and anthropogenic factors. *Science*, *285*(5433), 1505-1510.

Harvell, D., Aronson, R., Baron, N., Connell, J., Dobson, A., Ellner, S., Gerber, L., Kim, K. Kuris, A., McCallum, H., Lafferty, K., McKay, B., Porter, J., Pascual M., Smith, G., Sutherland, K., & Ward, J. (2004). The rising tide of ocean diseases: unsolved problems and research priorities. *Frontiers in Ecology and the Environment*, *2*(7), 375-382.

Hayes, R. L., & Goreau, N. I. (1998). The significance of emerging diseases in the tropical coral reef ecosystem. *Rev. Biol. Trop*, *46*(Supl 5), 173-185.

Heikoop, J. M., Dunn, J. J., Risk, M. J., Sandeman, I. M., Schwartz, H. P., & Waltho, N. (1998). Relationship between light and the δ15N of coral tissue: examples from Jamaica and Zanzibar. *Limnology and Oceanography*, *43*(5), 909-920.

Heikoop, J. M., Dunn, J. J., Risk, M. J., Schwarcz, H. P., McConnaughey, T. A., & Sandeman, I. M. (2000). Separation of kinetic and metabolic isotope effects in carbon-13 records preserved in reef coral skeletons. *Geochimica et Cosmochimica Acta*, *64*(6), 975-987.

Heikoop, J. M., Risk, M. J., Lazier, A. V., Edinger, E. N., Jompa, J., Limmon, G. V., Dunn, J. J., Browne, D. R., & Schwarcz, H. P. (2000). Nitrogen-15 signals of anthropogenic nutrient loading in reef corals. *Marine Pollution Bulletin*, *40*(7), 628-636.

Helmchen F., & Denk, W. (2005). Deep tissue two-photon microscopy. Nat. Methods. 2, 932-940.

Highsmith, R. C. (1979). Coral growth rates and environmental control of density banding. *Journal of Experimental Marine Biology and Ecology*, *37*(2), 105-125.

Hoegh-Guldberg, O. (1999). Climate change, coral bleaching and the future of the world's coral reefs. *Marine and freshwater research*, *50*(8), 839-866.

Hoegh-Guldberg, O., & Smith, G. J. (1989). The effect of sudden changes in temperature, light and salinity on the population density and export of zooxanthellae from the reef corals Stylophora pistillata Esper and Seriatopora hystrix Dana. *Journal of Experimental Marine Biology and Ecology*, *129*(3), 279-303.

Hoegh-Guldberg, O., Mumby, P. J., Hooten, A. J., Steneck, R. S., Greenfield, P., Gomez, E., Harvell, C. D., Sale, P. F., Edwards, A. J., Caldeira, K., Knowlton, N., Eakin, C. M., Iglesias-Prieto, R., Muthiga, N. Bradbury, R. H., Dubi, A., & Hatziolos, M. E. (2007). Coral reefs under rapid climate change and ocean acidification. *science*, *318*(5857), 1737-1742.

Holcomb, M., Venn, A. A., Tambutte, E., Tambutte, S., Allemand, D., Trotter, J., & McCulloch, M. (2014). Coral calcifying fluid pH dictates response to ocean acidification. *Scientific reports*, *4*.

Houlbreque, F., & Ferrier-Pagès, C. (2009). Heterotrophy in tropical scleractinian corals. *Biological Reviews*, *84*(1), 1-17.

James, Noel P. (1978). Facies Models 10. Reefs. *Geoscience Canada* 5.1

Jones, R. J., Bowyer, J., Hoegh-Guldberg, O., & Blackall, L. L. (2004). Dynamics of a temperature-related coral disease outbreak. *Marine Ecology Progress Series*,*281*, 63-77.

Kaczmarsky, L. T., Draud, M., & Williams, E. H. (2005). Is there a relationship between proximity to sewage effluent and the prevalence of coral disease. *Caribb J Sci*, *41*(1), 124-137.

Kingsley, R. J., & Watabe, N. (1985). An autoradiographic study of calcium transport in spicule formation in the gorgonian Leptogorgia virgulata (Lamarck)(Coelenterata: Gorgonacea). *Cell and tissue research*, *239*(2), 305-310.

Kim, K., & Harvell, C. D. (2002). Aspergillosis of sea fan corals: disease dynamics in the Florida Keys. *The Everglades, Florida Bay, and coral reefs of the Florida Keys: an ecosystem sourcebook*, 813-824.

Klaus, J. S., Frias-Lopez, J., Bonheyo, G. T., Heikoop, J. M., & Fouke, B. W. (2005). Bacterial communities inhabiting the healthy tissues of two Caribbean reef corals: interspecific and spatial variation. *Coral Reefs*, *24*(1), 129-137.

Klaus, J. S., Janse, I., Heikoop, J. M., Sanford, R. A., & Fouke, B. W. (2007). Coral microbial communities, zooxanthellae and mucus along gradients of seawater depth and coastal pollution. *Environmental microbiology*, *9*(5), 1291-1305.

Knowlton, N. (2001). The future of coral reefs. *Proceedings of the National Academy of Sciences*, *98*(10), 5419-5425.

Knowlton, N., & Budd, A. F. (2001). Recognizing coral species present and past.*Evolutionary Patterns. Growth Form, and Tempo in the Fossil Record. University of Chicago Press, Chicago*, 97-119.

Knowlton, N., Weil, E., Weigt, L. A., & Guzmán, H. M. (1992). Sibling species in Montastraea annularis, coral bleaching, and the coral climate record.*Science(Washington)*, *255*(5042), 330-333.

Knutson, D. W., Buddemeier, R. W., & Smith, S. V. (1972). Coral chronometers: seasonal growth bands in reef corals. *Science*, *177*(4045), 270-272.

Kuta, K., & Richardson, L. (2002). Ecological aspects of black band disease of corals: relationships between disease incidence and environmental factors. *Coral Reefs*, *21*(4), 393-398.

Leder, J. J., Swart, P. K., Szmant, A. M., & Dodge, R. E. (1996). The origin of variations in the isotopic record of scleractinian corals: I. Oxygen. *Geochimica et Cosmochimica Acta*, *60*(15), 2857-2870.

Lipp, E. K., Jarrell, J. L., Griffin, D. W., Lukasik, J., Jacukiewicz, J., & Rose, J. B. (2002). Preliminary evidence for human fecal contamination in corals of the Florida Keys, USA. *Marine Pollution Bulletin*, *44*(7), 666-670.

Logan, C. A., Dunne, J. P., Eakin, C. M., & Donner, S. D. (2014). Incorporating adaptive responses into future projections of coral bleaching. *Global change biology*, *20*(1), 125-139.

Longman, Mark W. (1981). A process approach to recognizing facies of reef complexes.

Lough, J. M., & Barnes, D. J. (1997). Several centuries of variation in skeletal extension, density and calcification in massive Porites colonies from the Great Barrier Reef: A proxy for seawater temperature and a background of variability against which to identify unnatural change. *Journal of Experimental Marine Biology and Ecology*, *211*(1), 29-67.

Loya, Y., Sakai, K., Yamazato, K., Nakano, Y., Sambali, H., & Van Woesik, R. (2001). Coral bleaching: the winners and the losers. *Ecology Letters*, *4*(2), 122-131.

Marshall, A. T., & Clode, P. (2004). Calcification rate and the effect of temperature in a zooxanthellate and an azooxanthellate scleractinian reef coral.*Coral Reefs*, *23*(2), 218-224.

Marubini, F., & Davies, P. S. (1996). Nitrate increases zooxanthellae population density and reduces skeletogenesis in corals. *Marine Biology*, *127*(2), 319-328.

McClanahan, T. R., Graham, N. A., & Darling, E. S. (2014). Coral reefs in a crystal ball: predicting the future from the vulnerability of corals and reef fishes to multiple stressors. *Current Opinion in Environmental Sustainability*, *7*, 59-64.

McWilliams, J. P., Côté, I. M., Gill, J. A., Sutherland, W. J., & Watkinson, A. R. (2005). Accelerating impacts of temperature-induced coral bleaching in the Caribbean. *Ecology*, *86*(8), 2055-2060.

Messenger, J. B. (2001). Cephalopod chromatophores: neurobiology and natural history. *Biological Reviews of the Cambridge Philosophical Society*, *76*(04), 473-528.

Miller, A. W., & Richardson, L. L. (2014). Emerging coral diseases: a temperature-driven process?. *Marine Ecology*.

Miller, J., Waara, R., Muller, E., & Rogers, C. (2006). Coral bleaching and disease combine to cause extensive mortality on reefs in US Virgin Islands. *Coral Reefs*,*25*(3), 418-418.

Muller, E. M., Rogers, C. S., Spitzack, A. S., & Van Woesik, R. (2008). Bleaching increases likelihood of disease on Acropora palmata (Lamarck) in Hawksnest Bay, St John, US Virgin Islands. *Coral Reefs*, *27*(1), 191-195.

Muscatine, L. (1980). Productivity of zooxanthellae. In *Primary productivity in the sea* (pp. 381-402). Springer US.

Muscatine, L., R McCloskey, L., & E Marian, R. (1981). Estimating the daily contribution of carbon from zooxanthellae to coral animal respiration1. *Limnology and oceanography*, *26*(4), 601-611.

Mydlarz, L. D., McGinty, E. S., & Harvell, C. D. (2010). What are the physiological and immunological responses of coral to climate warming and disease?. *The Journal of experimental biology*, *213*(6), 934-945.

Mydlarz, L. D., Couch, C. S., Weil, E., Smith, G., & Harvell, C. (2009). Immune defenses of healthy, bleached and diseased Montastraea faveolata during a natural bleaching event. *Diseases of aquatic organisms*, *87*(1-2), 67-78.

Nowack, E. C., Melkonian, M., & Glöckner, G. (2008). Chromatophore genome sequence of Paulinella sheds light on acquisition of photosynthesis by eukaryotes.*Current Biology*, *18*(6), 410-418.

Palmer, C. V., Bythell, J. C., & Willis, B. L. (2010). Levels of immunity parameters underpin bleaching and disease susceptibility of reef corals. *The FASEB Journal*, *24*(6), 1935-1946.
Peters, E. C. (1984). A survey of cellular reactions to environmental stress and disease in Caribbean scleractinian corals. *Helgoländer Meeresuntersuchungen*,*37*(1-4), 113-137.

Pandolfi, J. M., Jackson, J. B. C., Baron, N., Bradbury, R. H., Guzman, H. M., Hughes, T. P., ... & Sala, E. (2005). Are U. S. Coral Reefs on the Slippery Slope to Slime?. *Science (Washington)*, 307(5716), 1725-1726.

Peters, E. C., & Pilson, M. E. (1985). A comparative study of the effects of sedimentation on symbiotic and asymbiotic colonies of the coral Astrangiadanae Milne Edwards and Haime 1849. *Journal of Experimental Marine Biology and Ecology*, *92*(2), 215-230.

Porter, J. W., Fitt, W. K., Spero, H. J., Rogers, C. S., & White, M. W. (1989). Bleaching in reef corals: physiological and stable isotopic responses. *Proceedings of the National Academy of Sciences*, *86*(23), 9342-9346.

Raes, M., De Troch, M., Ndaro, S. G. M., Muthumbi, A., Guilini, K., & Vanreusel, A. (2007). The structuring role of microhabitat type in coral degradation zones: a case study with marine nematodes from Kenya and Zanzibar. *Coral Reefs*, *26*(1), 113-126.

Reading, H. G., & Collinson, J. D. (1996). Clastic coasts. *Sedimentary environments: processes, facies and stratigraphy*, 154-231.

Reading, H. G. (Ed.). (2009). *Sedimentary environments: processes, facies and stratigraphy*. John Wiley & Sons.

Reynaud, S., Ferrier-Pages, C., Meibom, A., Mostefaoui, S., Mortlock, R., Fairbanks, R., & Allemand, D. (2007). Light and temperature effects on Sr/Ca and Mg/Ca ratios in the scleractinian coral Acropora sp. *Geochimica et Cosmochimica Acta*, *71*(2), 354-362.

Rohwer, F., Seguritan, V., Azam, F., & Knowlton, N. (2002). Diversity and distribution of coral-associated bacteria. *Marine Ecology Progress Series*,*243*(1)

Rohwer, F., Breitbart, M., Jara, J., Azam, F., & Knowlton, N. (2001). Diversity of bacteria associated with the Caribbean coral Montastraea franksi. *Coral Reefs*,*20*(1), 85-91.

Rosenberg, E., & Ben-Haim, Y. (2002). Microbial diseases of corals and global warming. *Environmental microbiology*, *4*(6), 318-326.

Rosenberg, E., Koren, O., Reshef, L., Efrony, R., & Zilber-Rosenberg, I. (2007). The role of microorganisms in coral health, disease and evolution. *Nature Reviews Microbiology*, *5*(5), 355-362.

Rowan, R., & Knowlton, N. (1995). Intraspecific diversity and ecological zonation in coral-algal symbiosis. *Proceedings of the National Academy of Sciences*, *92*(7), 2850-2853.

Salih, A., Larkum, A., Cox, G., Kühl, M., & Hoegh-Guldberg, O. (2000). Fluorescent pigments in corals are photoprotective. *Nature*, *408*(6814), 850-853.

Salih, A., Wiedenmann, J., Matz, M., Larkum, A. W., & Cox, G. (2006, February). Photoinduced activation of GFP-like proteins in tissues of reef corals. In *Biomedical Optics 2006* (pp. 60980B-60980B). International Society for Optics and Photonics.

Schlichter, D., Meier, U., & Fricke, H. W. (1994). Improvement of photosynthesis in zooxanthellate corals by autofluorescent chromatophores. *Oecologia*, *99*(1-2), 124-131.

Schlichter, D., Weber, W., & Fricke, H. W. (1985). A chromatophore system in the hermatypic, deep-water coral Leptoseris fragilis (Anthozoa: Hexacorallia).*Marine Biology*, *89*(2), 143-147.

Schlichter, D., Fricke, H. W., & Weber, W. (1986). Light harvesting by wavelength transformation in a symbiotic coral of the Red Sea twilight zone. *Marine Biology*,*91*(3), 403-407.

Shashar, N., Banaszak, A. T., Lesser, M. P., & Amrami, D. (1997). Coral endolithic algae: life in a protected environment. *Pacific Science*, *51*(2), 167-173.

Shnit-Orland, M., & Kushmaro, A. (2009). Coral mucus-associated bacteria: a possible first line of defense. *FEMS microbiology ecology*, *67*(3), 371-380.

Sivaguru, M., Fried, G. A., Miller, C. A., & Fouke, B. W. (2014). Multimodal Optical Microscopy Methods Reveal Polyp Tissue Morphology and Structure in Caribbean Reef Building Corals. *JoVE (Journal of Visualized Experiments)*, (91), e51824-e51824.

Sivaguru, M., Mander, L., Fried, G., & Punyasena, S. W. (2012). Capturing the surface texture and shape of pollen: a comparison of microscopy techniques. *PloS one*, *7*(6), e39129.

Spalding, M., Ravilious, C., & Green, E. P. (2001). *World atlas of coral reefs*. Univ of California Press.

Stanley, G. D. (Ed.). (2001). *The history and sedimentology of ancient reef systems* (Vol. 17). Springer Science & Business Media.

Stanley Jr, G. D., & Swart, P. K. (1995). Evolution of the coral-zooxanthenllae symbiosis during the Triassic: A geochemical approach. *Paleobiology*, 179-199.

Stanley, G. D. (2003). The evolution of modern corals and their early history.*Earth-Science Reviews*, *60*(3), 195-225.

Sulvaran, G. (2014, May 2). Vernieuwing waterzuiceringsinstallatie Klein Hofje noodzakelijk. *Amigoe.* Retrieved from http://www.kkcuracao.info/.

Swart, P. K. (1983). Carbon and oxygen isotope fractionation in scleractinian corals: a review. *Earth-Science Reviews*, *19*(1), 51-80.

Swart, P. K., Saied, A., & Lamb, K. (2005). Temporal and spatial variation in the δ15N and δ13C of coral tissue and zooxanthellae in Montastraea faveolata collected from the Florida reef tract. *Limnology and Oceanography*, *50*(4), 1049-1058.

Swart, P. K., Leder, J. J., Szmant, A. M., & Dodge, R. E. (1996). The origin of variations in the isotopic record of scleractinian corals: II. Carbon. *Geochimica et Cosmochimica Acta*, *60*(15), 2871-2885.

Swart, P. K., Szmant, A., Porter, J. W., Dodge, R. E., Tougas, J. I., & Southam, J. R. (2005). The isotopic composition of respired carbon dioxide in scleractinian corals: implications for cycling of organic carbon in corals.*Geochimica et Cosmochimica Acta*, *69*(6), 1495-1509.

Szmant, A. M., Weil, E., Miller, M. W., & Colon, D. E. (1997). Hybridization within the species complex of the scleractinan coral Montastraea annularis. *Marine Biology*, *129*(4), 561-572.

Tambutté, É., Allemand, D., Mueller, E., & Jaubert, J. (1996). A compartmental approach to the mechanism of calcification in hermatypic corals.*The Journal of experimental biology*, *199*(5), 1029-1041.

Thornhill, D. J., Rotjan, R. D., Todd, B. D., Chilcoat, G. C., Iglesias-Prieto, R., Kemp, D. W., LaJeunesse, T. C., Reynolds, J. M., Schmidt, G. W., Shannon, T. Warner, M. E. & Fitt, W. K. (2011). A connection between colony biomass and death in Caribbean reef-building corals. *PLoS One*, *6*(12), e29535.

Toller, W. W., Rowan, R., & Knowlton, N. (2001). Repopulation of zooxanthellae in the Caribbean corals Montastraea annularis and M. faveolata following experimental and disease-associated bleaching. *The Biological Bulletin*, *201*(3), 360-373.

Trench, R. K. (1971). The Physiology and Biochemistry of Zooxanthellae Symbiotic with Marine Coelenterates. II. Liberation of Fixed ^{14}C by Zooxanthellae in vitro. *Proceedings of the Royal Society of London. Series B. Biological Sciences*, *177*(1047), 237-250.

Van Duyl, F. C. (1985). Atlas of the Living Reefs of Cura «; ao and Bonaire (Netherlands Antilles). *Foundation for Scientific Research in Surinam and the Netherlands Antilles*, *117*.

Vermeij, M. J., Van Moorselaar, I., Engelhard, S., Hörnlein, C., Vonk, S. M., & Visser, P. M. (2010). The effects of nutrient enrichment and herbivore abundance on the ability of turf algae to overgrow coral in the Caribbean. *PLoS One*, *5*(12), e14312.

Voss, J. D., & Richardson, L. L. (2006). Nutrient enrichment enhances black band disease progression in corals. *Coral Reefs*, *25*(4), 569-576.

Walker, D. I., & Ormond, R. F. G. (1982). Coral death from sewage and phosphate pollution at Aqaba, Red Sea. *Marine Pollution Bulletin*, *13*(1), 21-25.

Wederfoort, Ronald. Effects of Dumping Sewage Water Directly Into the Sea. Curacao Caribbean, & International Compliance Solution. Curacao Intelligence Service. Jan. 2015.

Wederfoort, Ronald. Pollution of the Ocean by Sewage (CURACAO), Nutrients, and Chemicals Curacao Caribbean, & International Compliance Solution. Curacao Intelligence Service. Jan. 2015.

Weil, E., & Knowton, N. (1994). A multi-character analysis of the Caribbean coral Montastraea annularis (Ellis and Solander, 1786) and its two sibling species, M. faveolata (Ellis and Solander, 1786) and M. franksi (Gregory, 1895). *Bulletin of Marine Science*, *55*(1), 151-175.

Wilson, J. L. (1974). Characteristics of carbonate-platform margins. *AAPG Bulletin*, *58*(5), 810-824.

Yang, H., Shen, J., Fu, F., Wang, Y., & Zhao, N. (2014). Black band disease as a possible factor of the coral decline at the northern reef-flat of Yongxing Island, South China Sea. *Science China Earth Sciences*, *57*(4), 569-578.